
THE APPLICATION OF MICROFLUIDICS TO CONTINUOUS WATER TOXICITY MONITORING

Emanuele Mele

A thesis submitted to Cardiff University in accordance with the requirements for the degree of Master of philosophy (Engineering).

Cardiff School of Engineering, May 2013



To my parents...

Acknowledgements

I would like to express my utmost appreciation to my supervisors Pr. David Barrow, Dr. Victoria Gray, Ms. Nicki Randles and Dr Oliver Puckering for their supportive guidance, advice and enthusiasm throughout the course of this research project.

I extend my gratitude to Cardiff University School of Engineering, Modern Water (MW), and the Knowledge Transfer Partnership (KTP) for funding this research project and offering me the opportunity to present this work at national and international conferences.

I must also thank Pr. David Lloyd and Bincy for giving me precious advice.

Many thanks go also to my colleagues, in particular to Lily, Nick, Alex, Jin and Erika for their support as well for their sincere friendship.

Many thanks go to my beloved friends Francesca, Stefania, Barbara, Erminia, Miri, Rafal and Justina, Lorenzo, Lydia and Michele, Luca and Melli, Paolo, Vincenzo, Henry, Diego and Chiara, Giancarlo, Magda, Adrian, Christos, Matteo, Maria, Ana, Marcus and Tomasz; their presence has made me feel less lonely and homesick.

Finally, I want to give particular thanks to my family, in particular to my mum, dad, brothers and girlfriend Alessandra for their immeasurable love, trust, encouragement and support that they provided me through every single day of my life. Without them, this work would not have been possible.

This work has been conducted in Cardiff University, School of Engineering and School of Biosciences, in collaboration with Modern Water (MW) and the Knowledge Transfer Partnership.

Abstract

The bioluminescence of certain marine bacteria (e.g., *Vibrio fischeri*), when in sufficient densities, provides a means by which the quality of water may be quantified as a whole organism response to harmful agents present within their microenvironment. This luminescence may be recorded by photodetectors, and the effects of toxic agents on the bacteria monitored as variations in light output. Such fundamental mechanisms are the basis for conventional water toxicity analysis instruments.

The development of a process by which the above analysis may be carried out in a continuous fashion has been successfully proven. The Continuous Toxicity Monitor (CTM), currently commercialised by Modern Water Ltd, is able to detect water toxicity in water and wastewater based on the above described mechanism thus acting as an early warning system.

Based on a predetermined set of initial requirements necessary to reduce the size of the system, and accordingly to the objectives of this research, it was carried an investigation that resulted in discrete number of improvements to the CTM.

Said set of discrete improvements, as an outcome of two years' worth of research on the development of a new water toxicity analyser "NANOTOX" are reported herein. These improvements represent the next stages of this development of the CTM as a miniaturized, planar microfluidic system using a polymer chip.

This new water toxicity analyser aspires to provide a solution to the critical need for a small, fast and more economical method to indicate the level of water toxicity. This could ultimately allows the deployment of continuous water toxicity monitoring in areas where such a need is paramount, such as (i) for water intake protection, (ii) effluent discharge and reuse, as well as, (iii) the treatment of water distribution systems.

Contents

CHAPTER 1.	General introduction.....	1
1.1	Overview.....	2
1.2	Water market analysis.....	3
1.3	Water quality analysis methods	5
1.4	The role of <i>Vibrio fischeri</i>	13
1.5	Setting up a bioreagent microbial culture of <i>Vibrio fischeri</i>	16
1.6	Introduction to the Continuous Toxicity Monitor (CTM).....	18
1.7	Project rationale	21
CHAPTER 2.	NANOTOX, technical developments	22
2.1	NANOTOX requirements	23
2.2	Viable material selection.....	27
2.3	Active microfluidic on NANOTOX, part I.....	29
2.3.1.	Conclusions.....	32
2.4	Active microfluidics on NANOTOX, part II	37
2.4.1.	Conclusion	43
2.5	Chilled <i>Vibrio fischeri</i> in substitution for a continuous microbial culture.	46
2.5.1.	Effect of chilled batch microbial culture of <i>Vibrio fischeri</i> in substitution for a continuous microbial culture and interaction with ZnSO ₄	49
2.5.2.	Results and conclusions	53
2.6	Use of stepped flow mixer (SFM) to enable the reduction of the differential pressure at mixing node 59	
2.7	Segmented flow test.....	68
2.7.1.	Results and conclusion.....	74
CHAPTER 3.	General discussion	81
3.1	Significance, limitation and future work.....	82

Annexes	86
---------------	----

List of Figures

Figure 1: <i>Vibrio fischeri</i> and microbial culture.	13
Figure 2: Hawaiian bobtail squid.	14
Figure 3: Image of an Anglerfish.	14
Figure 4: Schematic of the Continuous Toxicity Monitor (CTM).	20
Figure 5: Schematic of NANOTOX.	24
Figure 6: Classification of the pumps.	33
Figure 7: Set up of the equipment for gas pressure pumping.	38
Figure 8: Graph of air pump with 22cm flow restrictors.	40
Figure 9: Air pump with 22cm flow restrictor (excerpt of graph in Figure 8 from 0 to 90hrs).	41
Figure 10: Air pump with 22cm flow restrictor (excerpt of graph in Figure 8 from 100 to 160hrs after vessel unloading).	42
Figure 11: Schematic of the configuration with microdispensing valve and the electronic feedforward system.	45
Figure 12: Improved schematic of NANOTOX.	47
Figure 13: Description of the main working mechanism with chilled bioreagent.	48
Figure 14: Schematic of the Continuous Toxicity Monitor (CTM) readapted for experiments with chilled bioreagent.	50
Figure 15: Photon counts of raw bioreagent and mixed solution with chilled bacteria in substitution for a continuous microbial culture in the CTM analyser .	54
Figure 16: Photon counts of raw bioreagent and mixed solution with chilled bacteria in substitution for a continuous microbial culture in the CTM analyser.	55
Figure 17: Effect of the ZnSO ₄ (2.5 mg/L) on the chilled batch microbial culture of <i>Vibrio fischeri</i> in substitution with a continuous microbial culture in the CTM analyser.	56
Figure 18: Percentage of inhibition with 2.5 mg/L ZnSO ₄ in the CTM analyser.	56
Figure 19: FEM model of a T-connection showing surface concentration of two different liquids (top) and pressure line graph along the horizontal duct (bottom).	60
Figure 20: Cross-sectional view of the Stepped Flow Mixer (SFM).	61
Figure 21: FEM model of SFM with three branches.	64
Figure 23: Equipment set up.	71
Figure 24: PTFE chip clamped in metal case.	72

Figure 25: Example of milled chip design in COC. _____	72
Figure 26: EMCCD camera view from central window of the clamped system in Figure 23. _____	75
Figure 27: Mean bioluminescence of bacteria across the duct section during laminar single-phase flow of bioreagent. _____	76
Figure 28: Mean bioluminescence of bacteria across the duct section during segmented flow with sunflower oil. _____	77
Figure 29: Mean bioluminescence of bacteria across the duct section during air/bioreagent segmented flow. _____	78

List of Tables

<i>Table 1: Examples of commercially available water quality monitor based on multi parameter sensors and measured parameters.</i>	<i>10</i>
<i>Table 2: Examples of commercially available water quality monitors based on live organisms and respective live organism and detection method.....</i>	<i>12</i>
<i>Table 3: Recipe of the microbial culture medium M18 for Vibrio fischeri: this recipe employs a commercially available nutrient broth (Oxoid CM0067).....</i>	<i>17</i>
<i>Table 4: Pre-set flow requirements for NANOTOX during the earliest stages of the project.</i>	<i>26</i>
<i>Table 5: Thermoplastics selection.....</i>	<i>27</i>
<i>Table 6: General classification of pumping mechanisms in microfluidics as function of the maximum back pressure and minimum volumetric fluid flow.</i>	<i>34</i>
<i>Table 7: Selection of pumping systems.....</i>	<i>35</i>
<i>Table 8: Equipment gas pressure pump.....</i>	<i>39</i>
<i>Table 9: Probed values and fluid flow rates.</i>	<i>44</i>
<i>Table 10: Details of pumps and tubing</i>	<i>51</i>
<i>Table 11: Thermoplastics selection.....</i>	<i>87</i>

Glossary

mg	Microgram-s
ml	Microlitre-s
mm	Micrometre-s
cm	Centimetre-s
mm	Millimetre-s
nm	Nanometer-s
min	Minute
sec	Second
h ν	Energy
P	Pressure
λ	Wavelength
gm	Grams
MW	Modern Water plc.
CTM	Continuous Toxicity Monitor
Microtox	Gold standard for toxicity testing sold by Modern Water (MW)
Microtox CTM	Improved version of the CTM
Vf	<i>Vibrio fischeri</i> , gram negative photobacteria
PMTs	Photo Multiplier Tube
O ₂	Oxygen
ml	Millilitre-s
n.a.	Not applicable
U	Units
FMNH ₂	Reduced riboflavin phosphate
RCHO	Long chain aliphatic aldehyde
RCOOH	Carboxylic acid compounds
H ₂ O	Water
Preamp gain	Preamplifier gain
NaCl	Common Salt
EM gain	Electromagnetic gain
Θ	Contact angle
UK	United Kingdom

KTP	Knowledge Transfer Partnership
UV	Ultraviolet
R ²	Squared correlation coefficient
N	Number of replicates
SFM	Stepped flow mixer
PFD	Process flow diagram
M18	Medium recipe 18
COC	Cyclic olefin copolymer
PTFE	Polytetrafluoroethylene
R	Correlation coefficient
PS	Polystyrene
CAD	Computer-Aided Design
PP	Polypropylene
PES	Polyethersulfone
PEEK	Polyetheretherketone
PE	Polyethylene
PC	Polycarbonate
PET	Polyethylene terephthalate
PTB	Polybutylene terephthalate
PAI	Polyamide-imide
POM	Polyoxymethylene
PVDF	Polyvinylidene fluoride
FEP	Fluorinated ethylene propylene
PFA	Perflouroalkoxy
PDMS	Polydimethylsiloxane
PMMA	Polymethylmethacrylate
l	Litre-s
Zn	Zinc
Zinc sulphate	ZnSO ₄
Bioreagent	Bacterial sample drawn from the microbial bioreactor
psi	Pound per square inch (0.068 Bar)
Bar	10 ⁵ Pa
Atm	Atmosphere (Unit)

$-\log[\text{H}^+]$	Measure of hydrogen Ion activity
Na_2HPO_4	Disodium hydrogen phosphate
nA	Nano-ampere
A	Ampere
Kcps	Kilo-cycles per second
$^{\circ}\text{C}$	Centigrade
Mppc	Multi photon pixel counter
V	Voltage
pF	Pico-Farad
nF	Nano-Farad
μF	Micro-Farad
Ω	Ohms
K	Kilo
NI	National Instruments
NaH_2PO_4	Sodium phosphate monobasic monohydrate
d_b	Bubble diameter
Γ	Interfacial tension
$^{\circ}\text{F}$	Fahrenheit
N	Fluid velocity
KPa	Kilo-Pascal
Q	Volumetric flow rate
A	Diameter
P	Density
EK	Electro-kinetic

CHAPTER 1. GENERAL INTRODUCTION

1.1 OVERVIEW

Society has become increasingly aware of the impact of industrialization on the planet (Inglehart 1995). The continuous release of carbon dioxide, the discharge of harmful chemicals and the growing water pollution have led to an increased demand for systems to monitor water contamination, environmental pollution, and contribute to the prevention of environmental disasters (Sullivan 2002).

To detect water quality it is necessary to identify relevant physical, chemical, and biological indicators relative to water. There are many systems able to perform qualitative detection of contaminants in water (Goel 2006) and some of them are based on the use of *Vibrio fischeri* (Xiao-li *et al.* 2008), a bioluminescent bacterium which exhibits a phenomenon known as Quorum Sensing (Stevens & Greenberg 1997).

This chapter describes how to establish a microbial culture of *Vibrio fischeri* (called hereafter bioreagent), and provides a description of the working principle of the Continuous Toxicity Monitor (CTM) manufactured by Modern Water.

Due the relatively high retail cost (~£50K) and the large dimension (~2m x 0,8m x 1m) of the CTM, Modern Water undertook a collaborative research project with Cardiff University to prototype a key subsystems of a smaller, simpler, and less expensive analytical system based upon the same principle of water quality assessment.

1.2 WATER MARKET ANALYSIS

The clean water market expands along with the global population (Brown 2004). It was estimated at over \$655 million in the 2010 and is expected to grow to over \$800 million in 2015, representing a considerable expansion of 26% every year (MarketLine 2012). The world drinking water and wastewater market are expected to reach \$27 billion in 2017 (Global Industry Analysts 2012). Countries where water scarcity represents an exponentially growing problem, such as China, Brazil, and India (Oki and Kanae 2006), increasingly require treatment methods to access safe drinkable water (Bremere *et al.* 2001).

As industrialization takes place water pollution increases (Susmita Dasgupta, Benoit Laplante 2002). The presence of pollution and contaminants within the water distribution network is already a well-known problem (Luoma *et al.* 2008; Ashbolt 2004). Various water treatment processes and devices for toxicity detection are commercially available to improve and control water drinkability (Vanrolleghem & Dae Sung 2003). Several reports have noted the continuous growing demand of water purifiers in India, China, Brazil, and Russia (Hoekstra & Chapagain 2006). As a matter of fact the global market for water treatment had grown at 7% per year between 2002 and 2007 and it is expected to increase its annual grow rate (Gross & Deneen 2005). Chinese's demand for water purifiers has grown impressively during the last years and it is expected to increase at the Compound Annual Growth Rate (CAGR) of 24% until 2018 as a consequence of the continuously growing population and the increasing demand for safe drinkable water (TechSci Research 2013).

Despite current treatment technologies that produce more than 0.7 Million kg of clean water (in 2011) there is still insufficient safe drinking water to satisfy the current

population (TechSci Research 2012). Forecasts estimate that by 2025, 5.5 Billion people, 2/3 of the population, will live in water distressed countries (Mc Neely 1997).

1.3 WATER QUALITY ANALYSIS METHODS

Water quality is defined as a value measurement of the quality of the water in direct relation to one or more biotic species, such as humans (Johnson *et al.* 1997). There are set standards on water quality. Government bodies provide rules stating limits for the amount of certain contaminants in water (United States Environmental Protection Agency 2012; Government of Wales 2010; World Health Organization 2011; EEC 1981).

Water quality may be categorised for the intended use, in particular:

- i. **Human consumption:** generally, microorganisms such as viruses, bacteria, and protozoa; inorganic contaminants (e.g., salt and metals); and chemicals (e.g., pesticides and herbicides) are considered contaminants for human consumption. Water purifiers are necessary to remove these contaminants before water is distributed to users;
- ii. **Industrial and domestic use:** water for industrial and domestic use has a low presence of minerals such as calcium and magnesium, often present in hard water, which reduce the effects of cleaning agents and are responsible to the development of calcium sulphate and calcium carbonate deposits in heaters and boilers (Babbitt & Doland 1955). Therefore, industrial quality water is generally softened before it is distributed to users. On the contrary, hard water is still used for human consumption since health issues have been linked to mineral insufficiencies in the soft water; and
- iii. **Environmental water quality:** water quality standards vary significantly due the environmental conditions, presence of humans in nearby areas, and associated ecosystems. Untreated waters have high presence of toxic substances that may represent hazards which affect wildlife and vegetation (Tchobanoglous & Schroeder 1985). Quality laws specify protection for recreational uses, fisheries, and ecosystem preservation.

To detect water quality it is necessary to identify some physical, chemical, and biological indicators, such as:

- temperature, commonly detected to determine the rate of biochemical reactions in the aquatic environment. Temperature can harm aquatic organism if outside certain thresholds;
- conductance;
- odour;
- colour;
- total suspended solids (TSS), commonly detected to estimate dissolved sodium chloride and nutrients (e.g. nitrides and phosphates);
- transparency/turbidity, commonly measured as responsible of light penetration and therefore effecting level of photosynthesis;
- taste;
- $-\log[\text{H}^+]$, commonly measured to evaluate the acidity of the water. Expected normal levels are usually between 6 and 8;
- oxygen, commonly measured as vital to aquatic life and necessary for cellular respiration;
- hardness, commonly measured as function of the Calcium and Magnesium ions presence in the analysed water (Ca^{2+} , Mg^{2+});
- nitrates, commonly measured as fundamental nutrient for aquatic plants and animals;
- surfactants, typically found in very low concentrations in unpolluted waters;
- heavy metals such as mercury (Hg), cadmium (Cd), arsenic (As), chromium (Cr), thallium (Tl), and lead (Pb);

- orthophosphates, typically found in very low concentration in unpolluted waters; and
- microorganisms (*Ephemeroptera*, *Plecoptera*, *E.coli*, *Coliform*, etc.).

Indicators derived from the above measured parameters are ultimately judged to evaluate a global water quality index indicative of the quality of the water.

Different analysis methods may be used to monitor water quality, including:

- **In-lab analysis:** samples are taken, preserved, transported, and analysed in laboratories. In-lab analysis is associated with several problems, such as cost, the inability to produce real-time results, and the preservation of samples.

Standard methods to analyse water and wastewater include:

- High Performance Liquid Chromatography (HPLC). This consists in an improved form of liquid chromatography using higher pressure. HPLC tubes separate ions or molecules dissolved in a solvent after interaction with an analyte. A detector detects separated compounds as they elute in the HPLC column. (Lindsay & Kealey 1987);
- Mass Spectrometry (MS). It is an analytic technique that consists in the identification of the spectra of the atoms comprising materials. MS analyses degrees of deflection of particles by a magnetic field to find their masses. In MS samples are vaporized and then ionized by means of an Electronic Beam. Consequentially to the collision with the Electronic Beam, samples are accelerated toward an analyser tube surrounded with a curved magnetic field which influences the charged particles pathway by different degrees in proportion to their mass to charge ratio. (Boggess 2001);
- Ion-Selective Electrodes (ISEs). This method consists of the evaluation of the $-\log[H^+]$ of water. It involves a set of electrodes that are able to convert

the activity of ions dissolved in a solution into an electrical potential. According to Nernst equation, this potential is directly proportional to the logarithm of the ionic activity. ISEs need to be constantly calibrated (e.g., every hour). Data obtained, even if continuous, are affected by interferences and drifts (e.g., by organic particles) (Umezawa *et al.* 2000); and

- Biochemical Oxygen Demand (BOD). This is a widely used chemical test to identify the quality of water or wastewater (Sawyer *et al.* 2003). This method consists of measuring the concentration of dissolved oxygen (DO) before and after an incubation period (usually 5 days), and adjusting the value with the sample corresponding dilution factor (Clesceri *et al.* 2005).
- **Automatic sample collection:** this may be achieved using auto-samplers and quality monitors to collect/detect water samples in a programmed fashion. Usually these systems are able to function for extended periods of time, are easily maintained and cost effective (O'Halloran *et al.* 2009). Often, devices for automatic sample collection allow data logging, processed data information, and provide an early stage alarm system. Descriptions of the two methods used for automatic sample collection are listed as follows:
 - **multi parameter sensors:** a discrete array of sensors is often used to monitor water quality. In this case, the identification of some physical, chemical, and biological indicators is performed through a set of sensors that, in most of the cases, are just adaptations of the laboratory methods (e.g., ISEs, amperometric thermistor, polarographic, calorimetric, spectral UV-Vis, photoelectrochemical sensors, photoionization detectors (PID)). The quality of water may be assessed through the combined readings of these devices (O'Halloran *et al.* 2009). Research has pushed towards the development of electronic tongues able to quantify the presence of heavy

metals in water, such as micro-electrode array with ppb level of recognition (Ju *et al.* 2011) and monolithically integrated array of sensors (e.g., K^+ , Na^+ , Ca^{2+} based independent ISFETs with photocurable gate membranes and platinum electrodes) (Marco *et al.* 2006). Electronic tongues may also monitor pesticides. A few examples of commercially available full water quality monitor devices based on multi parameter sensors are given in Table 1. Electronic tongues and electronic noses might be applied, in the future and if further developed, as alternative methods to broad water quality monitors (O'Halloran *et al.* 2009).

Table 1: Examples of commercially available water quality monitor based on multi parameter sensors and measured parameters.

Production company and respective water quality monitor	Parameters measured by the water quality monitor sold by the company
Company name: scan Messtechnik GmbH Company website: http://www.s-can.at/ Water quality monitor sold by the Company: micro::station and nano:station	Colour, COD, BOD, Nitrate, Hydrogen sulphide, Potassium ions, pH, Oxidation reduction potential, O ₂ , Conductivity, Temperature, Hydrocarbon
Company name: Ecotech Pty Ltd Company website: http://www.ecotech.com Water quality monitor sold by the Company: Tethys: UV500 On Line Water Analyser	Ammonia, COD, NH ₄ , K ⁺ , Hydrocarbons, Phenol and BTEX, Chlorophyll A, Colour, Turbidity, pH, Dissolved oxygen, Conductivity
Company name: Stevens water Company website: http://www.stevenswater.com Water quality monitor sold by the Company: HYDROLAB MS5/DS5	Ammonia/Ammonium, Nitrate, Phosphorous, Nitrogen, Carbon

- **Live organisms monitors:** live organisms monitors which use common physicochemical and chemical tests, such as multi-parameters sensors, are limited by the chemical indicators chosen to determine the presence of toxic substances causing environmental pollution, within a solution (Roig *et al.*

2007). The intense development of new bio-analytical techniques which employ live organisms (e.g., mussels, *Daphnia*, and algae) (Borcherding & Wolf 2001; De Hoogh 2006; Ren *et al.* 2007) has characterised the last decade (Vanrolleghem, 2002). Monitors based on microorganisms (e.g., *Vibrio fischeri*), where the detection sensitivity depends by the interaction of living micro-organisms with the contaminants in water (Stolper *et al.* 2008), are alternative methods of detecting toxicity. Toxicity may be characterized by estimating the damage that contaminants may cause to live organisms (Ian *et al.* 2006). Therefore, the minimum requirements to detect toxicity with a live organism biomonitor are (1) a live organism (2) one or more parameters to indicate the state of health of the microorganism (3) a measurement method to identify these physiological parameters (Bulich, 1979).

Live organism biomonitoring detects a wide range of contaminants, which affect the health of the living organism. However, there is no clear link between the harm to living organisms and the hazard for humans (e.g., genotoxicants and endocrine disruptors). In addition to that, biomonitoring based on living organisms may only identify high toxicity and not chronic toxicity; pollutants provoking chronic effects may be recognized with laboratory-based *in vitro* assays (Flückiger-Isler *et al.* 2004; Sonneveld *et al.* 2005; Eltzov *et al.* 2009). Therefore, to get a broad detection of contaminants together with few individual results related to few specific water quality parameters, a tailored combination of multi-parameter sensors and monitors based on living organisms is required.

Table 2: Examples of commercially available water quality monitors based on live organisms and respective live organism and detection method

Production company and respective water quality monitor	Detected live organism and respective method of detection
<p>Company name: Modern Water plc</p> <p>Company website: http://www.modernwater.com/</p> <p>Water quality monitor sold by the Company:</p> <p style="text-align: center;">Continuous water toxicity monitor (CTM)</p>	<p><i>Vibrio fischeri</i> using PMT</p>
<p>Company name: Liquid Analytical Resource, LLC</p> <p>Company website: http://larllc.com/</p> <p>Water quality monitor sold by the Company:</p> <p style="text-align: center;">Nitritox</p>	<p>Nitrifying bacteria using fluorimeters</p>
<p>Company name: CheckLight Ltd</p> <p>Company website: http://www.checklight.biz/</p> <p>Water quality monitor sold by the Company:</p> <p style="text-align: center;">CheckLight BIOmonitor</p>	<p><i>Vibrio fischeri</i> using PMT</p>

1.4 THE ROLE OF *VIBRIO FISCHERI*

Vibrio fischeri (Figure 1) is commonly found throughout the oceans of the world (Madigan 2005). They have evolved to utilise their bioluminescence as a means of communication (Swift *et al.* 1996). They exist in a symbiotic relationship with other living creatures (Ruby *et al.* 2005), such as the Hawaiian bobtail squid (*Euprymna scolopes*) (Figure 2).

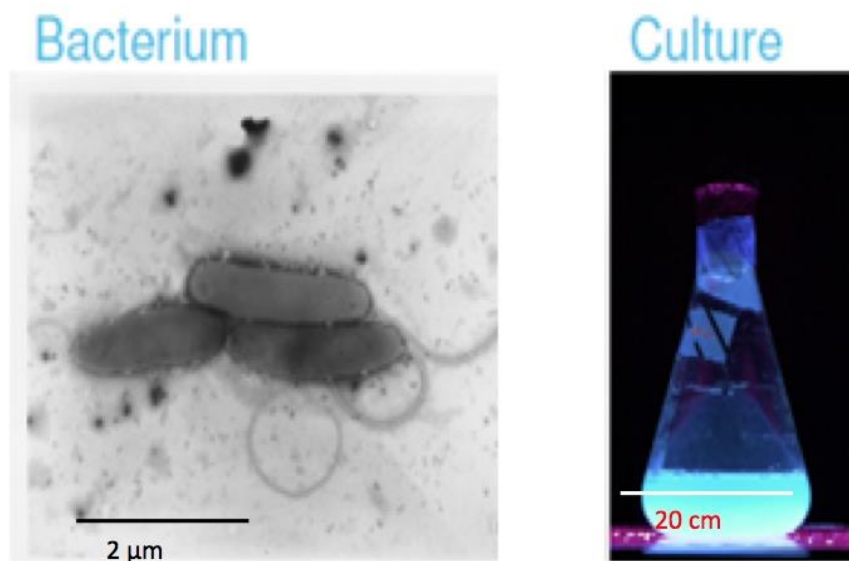


Figure 1: *Vibrio fischeri* and microbial culture: bacterium (left), three *Vibrio fischeri* swimming in a microbial culture medium; the pilus (hair-like appendix used by bacteria for conjugation) of the three bacteria is clearly visible. Photo was taken using scanning electron microscopy. Microbial culture of *Vibrio fischeri* in a Duran flask (right); blue light is emitted from bacteria. Image was taken with a DSLR camera in a dark room.

Evolution has enabled some organisms (e.g., Hawaiian bobtail squid (*Euprymna scolopes*)) to use bacteria that emit light as a camouflage to remove its shadow on the sea floor (Jereb *et al.* 2005). Also, others, such as the Anglerfish (*Lophiiformes*), a carnivorous fish that is commonly found in the Atlantic Ocean (Figure 3), uses *Vibrio fischeri* as a luminous, built-in bait to catch their prey when they are nearby (Crozier 1985).

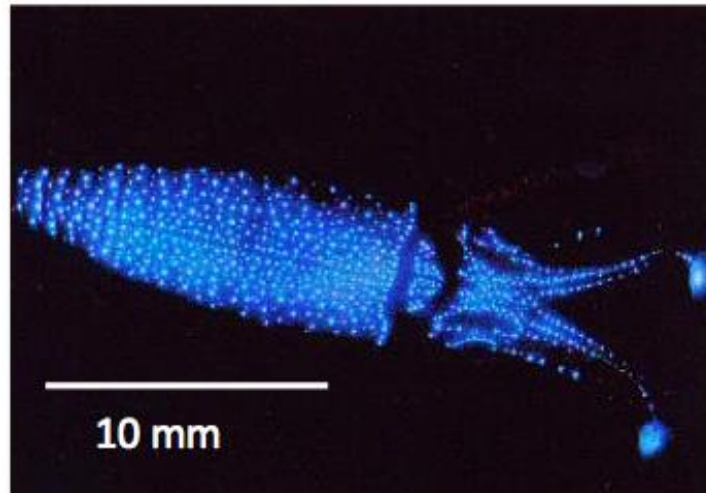


Figure 2: Hawaiian bobtail squid (figure reproduced from SeedsofRainbox, 2011): this is a species of bobtail squid commonly found in the Pacific Ocean. They grow up to 30mm in length and weight up to 2.67g. Photo shot was taken in the dark. The Hawaiian bobtail squid uses extra ocular vesicles in collaboration with its eyes as a light sensor, and modifies its ink sac to regulate the light of the *Vibrio fischeri*. This useful mechanism gives it the ability to remove its shadow from the sea floor. Moreover, the light organs comprise a network of reflectors distributed all over the body with the aim of distributing light throughout the mantle.



Figure 3: Image of an Anglerfish: their distinctive feature is the dorsal spine that protrudes above the mouth acting as a fishing pole. Anglerfish are carnivores; they may weigh up to 50kg, and are from 20cm to 1m in length. There are more than 200 species and most of them live in the Atlantic Ocean. Photograph courtesy of Bruce Robison/Corbis, National geographic.

Vibrio fischeri generate visible light as consequence of a chemical reaction in response to an outer stimuli. This phenomenon is known as ‘Quorum Sensing’ and appears when the population density reaches a threshold density (Stevens and Greenberg 1997). At this density the external molecular auto-inducer, N-(3-oxohexanoyl)-homoserine lactone, triggers a reaction (Eberhard *et al.* 1981). The auto-inducer is produced in the cytoplasm of the bacterium and released into the extracellular environment (Engebrecht and Silverman 1984). The chemical reaction that occurs is described in equation 1.

Specifically, the reaction described above comprises oxidation of long-chain aliphatic aldehyde (RCHO) and a reduced flavin mononucleotide (FMNH₂). The reaction generates luciferin (FMN), the oxidized form of the aldehyde, and water. The residual energy is released in form of blue-green visible light at 490nm. In conclusion, the reaction reflects the total health of the micro-organism (Eberhard *et al.* 1981).

Equation 1: (Wilson (1998)).



1.5 SETTING UP A BIOREAGENT MICROBIAL

CULTURE OF *VIBRIO FISCHERI*

Setting up a new microbial culture of *Vibrio fischeri* will require the preparation of the nutrient (microbial culture medium) to sustain the growth of the microorganisms (Haderl *et al.* 1995). A microbial culture medium was prepared in two conical flasks of 500ml each, using a commercially available nutrient broth (Oxoid CM0067) as reported in Table 3.

Oxoid CM0067 is a nutritious medium suitable for the cultivation of micro-organisms. Oxoid CM0079 typical formula comprises 'Lab-Lemco' powder 10.0 gm/litre, Peptone 10.0 gm/litre, Sodium chloride gm/litre 5.0. 'Lab-Lemco' is a refined meat extract.

The flasks were autoclaved at a temperature of 121°C for 20 minutes and allowed to cool before inoculation. After that, the flasks were inoculated with frozen *Vibrio fischeri* (NRL 11177) from a pure photobacterium agar plate microbial culture. The microbial flasks were incubated in a reciprocating shaker (Gallenkamp) at ambient temperature (~22°C), and shaking at 80rpm for 24-48hrs. After this period the microbial culture was ready and the bioluminescence was visibly observable, giving a clear indication of the good status of the bacteria.

Table 3: Recipe of the microbial culture medium M18 for *Vibrio fischeri*: this recipe employs a commercially available nutrient broth (Oxoid CM0067).

Compound	Quantity
NaCl	23g
Na ₂ HPO ₄	15.5g
NaH ₂ PO ₄	2.0g
Nutrient broth #2 (Oxoid CM0067)	10g
Distilled Water	1litre

1.6 INTRODUCTION TO THE CONTINUOUS TOXICITY MONITOR (CTM)

The Continuous Toxicity Monitor (CTM), sold by MW (Modern Water 2010), is able to detect water toxicity in water and wastewater acting as an early warning system (Liu *et al.* 2010). Its working mechanism is represented in Figure 4. The CTM measures changes of light (inhibition) between healthy bacteria and bacteria exposed to toxins enabling an automatic and real-time detection of a large range of water contaminants such as metals, herbicides, fungicides, solvents, and algal toxins (Randles 2010).

As provided in Figure 4 blank solution is used to obtain a first response, a baseline L_B , from light detector PMT (L_1) and thus calibrate the system to further establish quality of the sample water with respect to the baseline. On the other hand, light detector PMT (L_0) provides status of health of raw bioreagent from the fermentor, prior to interaction with sample water at mixing node.

The inhibition is defined in the following relationship:

Equation 2: Inhibition

$$INHIBITION (\%) = \frac{L_B - L_1}{L_B} \times 100$$

where:

- L_B is the light output after exposure with blank solution; and
- L_1 is the light output after exposure with sample water (2 minutes after exposure).

Temperature influences health status of the bacteria, thereby causing variation of the light output. As such, analyte should be maintained at stable temperature ($\sim 22^\circ\text{C}$) at detection of

light output. In CTM bioreagent is maintained at all time at $\sim 22^{\circ}\text{C}$ to keep bacteria in ideal conditions, even after interaction with sample water.

As some contaminants in the sample water may need longer time to interact with bioreagent, an additional PMT (L_2) may be used to get a response against a broader range of contaminants. The additional PMT (L_2) tests the bioluminescence at 5 minutes after the exposure with the sample water.

Accordingly with this description, same PMT model and same conditions are used for all the PMTs of the CTM. The only difference is the location of detection.

When inhibition is greater than a pre-set value an alarm condition may be triggered. Water and/or wastewater, in their normal conditions, will produce an inhibition even in the absence of toxicity when tested with the CTM. This is called background toxicity. An alarm condition is triggered by toxicity outside the normal range and abnormally fast changes in toxicity. For this reason, knowing the background toxicity is crucial. The CTM provides constant monitoring of background toxicity, providing essential data as well as protection against contamination events (Modern Water 2010a).

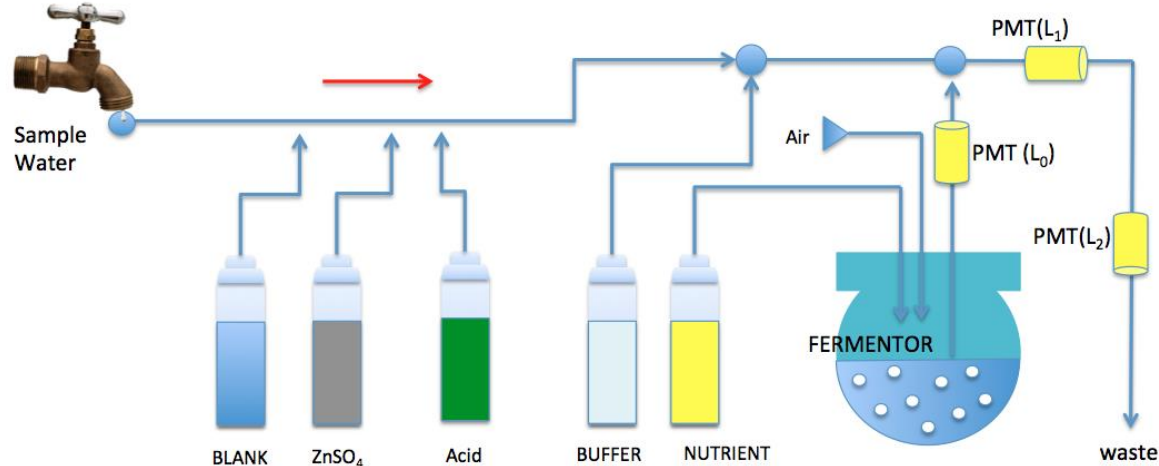


Figure 4: Schematic of the Continuous Toxicity Monitor (CTM): during normal working condition, the CTM continuously harvests bioluminescent bacteria (bioreagent) from a continuous microbial culture bioreactor (fermentor), mixes them with sample water (collected from the sample source) and brine (buffer) to dilute the bioreagent and allow reaction. The microbial bioreactor is constantly fed with a microbial culture medium (M18). It is aerated, stirred, and electronically controlled to maintain the expected growing condition and stable temperature at $\sim 22^{\circ}\text{C}$. Light output is measured using photomultiplier tubes (PMTs), 2 and 5 minutes after mixing point. This mechanism allows automatic and real-time detection of contaminants in water. The reagent section comprises a vessel with distilled water (BLANK) used to set a baseline light output from which inhibition may be evaluated. A calibrant solution (zinc sulphate (ZnSO_4)) is used to perform daily standard toxicity tests with known concentration (10ppm ZnSO_4). Cleaning reagent, such as citric acid (Acid) is used for daily cleaning procedure. The waste section comprises a waste tank.

1.7 PROJECT RATIONALE

The high cost and large dimension of the CTM, the critical need for a faster and more economical way that will allow real-time water toxicity monitoring, and the growing market for water quality monitors (Maxwell 2012) are the main reasons that led Modern Water and Cardiff University toward the realization of a miniaturised water toxicity analyser.

Microfluidic systems are ideally suited to answer these critical needs and offer many other advantages to broad water quality monitors. These systems have become appealing platforms for diagnostic applications and may be applied to reduce the dimension of detection devices (Eicher & Merten 2011).

The objective of this work is to provide a list of technical results as an outcome of two years' worth of research on the development of a new water toxicity analyser, "NANOTOX", based on an integrated microfluidic analytical system and on a disposable/sterilizable polymer with clear controls and data logging.

CHAPTER 2. NANOTOX, TECHNICAL DEVELOPMENTS

2.1 NANOTOX REQUIREMENTS

As described in the previous chapter, the Continuous Toxicity Monitor (CTM) is an expensive and heavy apparatus that provides continuous monitoring of water toxicity and protection against contamination events.

Figure 5 shows a simple schematic of NANOTOX, without reagent section (e.g., blank solution, cleaning reagent, and calibrating reagent), in accordance with the predefined requirements provided by Modern Water at the earliest stages of this project.

As provided in Figure 5, blank solution (not shown) is used to obtain a first response from light detector 1 and thus calibrate the system to further establish quality of the sample water. On the other hand, light detector 0 provides status of health of raw bioreagent from the fermentor, prior to interaction with sample water at mixing node.

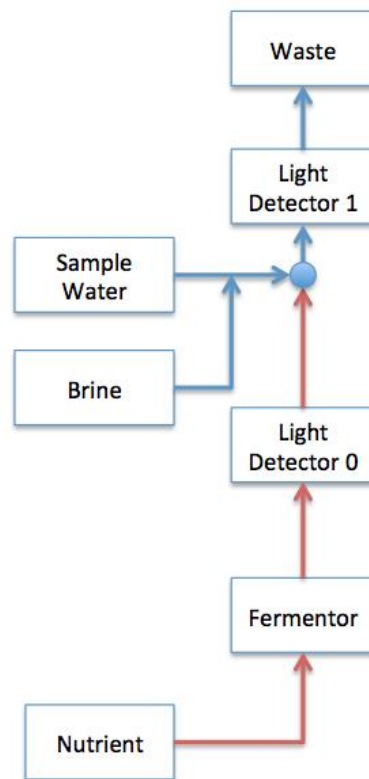


Figure 5: Schematic of NANOTOX: the device continuously harvests bioluminescent bacteria (bioreagent) from a microbial culture bioreactor (fermentor) and mixes them with sample water, and brine. It measures changes of light and allows automatic and real-time detection of contaminants in water. The microbial bioreactor is constantly fed with a microbial culture medium (Nutrient). It is aerated, stirred, and electronically controlled to maintain the expected growing condition. Light output is measured using photomultiplier tubes (PMTs). The microbial bioreactor is sterile. The red arrows shown in the figure represent sterile and antibacterial connections which prevent any bacterial contamination from growing back into the fermentor or into the nutrient section.

According to the initial requirements, NANOTOX includes a microbial bioreactor that keeps bacteria inside ideal conditions to preserve them for a long storage period. This could be obtained by keeping temperature close to an ideal value (21-24°C), by controlling aeration, by maintaining continuous stirring, and by keeping pressure close to ambient pressure. Other requirements comprise: the flow of the culture medium into the microbial bioreactor equal to the flow of bioreagent out of the microbial bioreactor to provide mass balance inside the microbial bioreactor and to maintain a continuous microbial culture; and

the use of a continuous, low cost, sterile, inert, and stable pumping system. Flow requirements were set as specified in Table 4.

Additionally, as further requirements, all wetted parts (e.g., microbial bioreactor, tubing, pumping system, and reservoirs) must:

- have an adequate chemical resistance to withstand chemical cleaning with an organic acid and/or mineral base, and disinfection with a halogen-based chemical disinfectant;
- be biocompatible (to preserve bacteria);
- have a low surface energy to reduce biofilm formation (Abu-Lail & Camesano 2006);
- be optically transparent, especially when in proximity of the PMTs, to allow photodetection;
- be amenable for mass production with standard methods of fabrication;
- be sterilizable (e.g., usually via heat and/or pressure);
- have a low water absorption; and
- be non-porous to avoid biofilm formation (Autumn *et al.* 2002).

Table 4: Pre-set flow requirements for NANOTOX during the earliest stages of the project. Reference is made to the schematic in Figure 5 in which the various components are shown along with arrows representing fluidic connections between components. Required flow rate values ($\pm 5\%$) for respective fluidic connections are shown in the table below. Accordingly, requirements for flow rates are 1:10 of the CTM flow rate.

Fluidic connection	Target flow rate value ($\pm 5\%$) for fluidic connection
From nutrient to fermentor	~7 $\mu\text{l}/\text{min}$
From brine to the mixing node with sample water.	~7 $\mu\text{l}/\text{min}$. Brine mixes at a ratio of 1:10 with sample Water. Accordingly, NaCl concentration in sample water and brine after mixture should be approximately 10 g/litre. Such condition is imposed to mimic sea water condition prior to interaction with bioreagent.
From fermentor to mixing node with sample water and brine. This is the bio-reagent outflow from the fermentor.	~7 $\mu\text{l}/\text{min}$. This is the bioreagent flow rate.
From sample water to the mixing node with brine.	~70 $\mu\text{l}/\text{min}$. 1:10 of the CTM flow rate.

2.2 VIABLE MATERIAL SELECTION

As defined in the requirement section (chapter 2.1), wet parts might be selected taking into account characteristics such as biocompatibility, low surface energy, sterilization, solvent resistance, and amenability to mass production. A list of the common thermoplastic materials along with their characteristics is provided in Table 11 in the Annexes section of this disclosure. Table 5 instead provides most prominent details of the 2 most attractive materials (COC, and FEP) per the requirements of paragraph 2.1. List in Table 11 was used as basis to select the material for the passive microfluidic chip (microfluidic pathway).

Table 5: Thermoplastics selection.

Name	Characteristics	Biocompatibility	Water θ (°)	Solvent resistant
Cyclic Olefin Copolymer (COC)	<ul style="list-style-type: none"> • Low density, • Excellent transparency (92%), • Low water absorption, • Biocompatible, • Good flowability, • Hydrophobicity, • Production by common hot embossing technique, • Surface energy may be changed by plasma treatment and remain modified for several days, • Sterilizable by autoclaving or gamma radiating, • Heat resistant. 	YES	85	Excellent

	(Shin <i>et al.</i> 2005; Fink 2010)			
Fluorinated ethylene propylene (FEP)	<ul style="list-style-type: none"> • FEP is softer than PTFE; • Highly transparent, • Resistant to sunlight, • Similar to PFA, • Sealable with thermobonding technique, but both temperature and pressure need cautious controls, • Little adsorption of biomolecules, • Difficult to thermobond. (Boedeker 2007)	YES	108	Excellent

According to the requirements in the previous chapter (Chapter 2.1), and the characteristics presented herein cyclic olefin copolymer (COC) was evaluated to be the most attractive material due its excellent transparency, good biocompatibility, its extremely low water absorption, its low surface energy, its amenability to sterilization procedures, and its amenability to mass production. FEP on the other end is a promising alternative if its thermobonding is improved.

2.3 ACTIVE MICROFLUIDIC ON NANOTOX, PART I

The active microfluidics refers to controlling and handling liquid flows by using active mechanisms such as pumps and valves. Pumps are used to supply liquids from a determined source to a system; they are responsible for temporal and volumetric fluid motion. Valves, instead, control the volumetric flow by temporarily opening and closing fluid passageway (Kirby 2009).

Pumps are classified into two principal groups (Laser & Santiago 2004): displacement pumps and dynamic pumps in accordance with Figure 6. Accordingly, displacement pumps work by reducing the internal boundaries of the confined liquid and force the fluid motion by applying pressure (e.g., syringe pumps, metering pumps, microdispensing pumps, peristaltic pumps, piezoelectric and annular gear pumps, etc.).

On the other hand, dynamic pumps apply forces directly to the fluid, without moving boundaries, such as magnetic fields, electric fields, centrifugal forces, and pressure variation to increase the momentum (e.g., venturi pump, centrifugal micropumps, gas pumps, electro-hydrodynamic pumps (EHD), magneto-hydrodynamic pumps (MHD), electrostatic pumps, and electro-osmotic pumps, etc.) (Qian and Bau 2009).

Displacement pumps are also classified into few categories based on the different tactics to pump liquids into microsystems. Categories are: reciprocating periodic pumps, such piston pumps, and diaphragm pumps; rotary periodic pumps employing gears, or vanes; and aperiodic displacement pumps.

The most common mechanisms used for pumping are diaphragm pumps. They are based on a physical actuator that drives fluid into microchannels by applying oscillatory or rotational pressure forces (Farideh *et al.* 2012). The physical actuator could be driven by either electrostatic forces applied to deflect the pump chambers, or piezoelectric effect by

coupling the mechanical deformation of a piezoelectric crystal with the electrical polarization, or electromagnetic actuation using coils to generate magnetic fields that produce attraction/repulsion of a permanent magnet that acts as a solenoid plunger, or thermopneumatic effect by heating and cooling the pump chambers in order to expand or contract their volume (Farideh Abhari 2012).

Thermo hydraulic pumps and piston pumps are commercially available e.g. by Cellnovo (UK). As an exemplary pump showing thermopneumatic effect, the thermo hydraulic pump sold by Cellnovo (UK) is provided with a semiconductor element immersed in the working medium and adjacent the diaphragm. Heating the working medium cause the medium to undergo the phase change into the liquid state, thereby expanding. Expansion and contraction of the expandable working medium causes a diaphragm to deflect (GB2443261B).

Piston-based pumping systems (e.g., metering pumps, microdispensing valves) are specific type of reciprocating displacement pumps. They are traditionally not used in the micro scale but in the macro scale. However, micro-fabricated valves may use pistons as evidenced by Kirby *et al.* (Kirby *et al.* 2002) to control fluid flow.

Dynamic pumps may be divided into few categories based on the forces applied to the pumped liquid. Those pumps are centrifugal pumps, typically ineffective at low Reynolds numbers; electro-hydrodynamic pumps (EHD), where the electric field acts directly with the working liquid; magneto-hydrodynamic pumps (MHD), where the electromagnetic field acts with the fluid; electroosmotic pumps (EO), where the surface charges developed within electrodes are responsible for the fluid flow; and miscellaneous pumps, such as jet effect (e.g., venturi pumps), and gas lift.

Electroosmotic pumps (EO) are also known as electrokinetic pumps. Conceptually, in EO pumps an electric field is applied parallel and proximal to an electric double layer (EDL).

EDL is a non-zero net charge region, typically a solid-liquid interface. The applied electric field affect motion of the surplus of electric charges in the EDL resulting in a net body force applied to the liquid in the nearby vicinity of the EDL.

Accordingly to the above, dynamic pumps that use magnetic or electric fields to drive liquids need specific working liquids to function properly and usually generate secondary effects (e.g., electrochemical reaction, generation of gases, heat by Joule effect) (Laser and Santiago 2004). These often represent a disadvantage that limits their usage for medical and biological applications especially when the working fluid contain bacteria susceptible to electric fields (Wu 2006).

2.3.1. CONCLUSIONS

Desired high backpressure and low fluid flow may be achieved with the commercially available pumping systems. Specifically, the pumps that may meet the requirements of the fluid flow for the nutrient and the bioreagent (Table 4) are microdispensing valves, syringe pumps, pressure gas pumps, EHD pumps, metering pumps, and annular gear pumps (Table 6). However, bacteria are susceptible to electric fields (Wu, 2006). For this reason dynamic pumps such as EHD, MHD, and EO pumps may not be applied. Therefore, only pressure gas pumps, syringe pumps, microdispensing pumps, metering pumps, and annular gear pumps may be used in this specific application.

Some microfluidic systems require internal self-contained micropumps of scale similar to the scale of the liquid's volume to be pumped (Karanth *et al.* 2010). This is not the case for the pumping systems applied in NANOTOX, which instead requires an external and commercially available pumping system. A set of commercially available pumping systems is provided in Table 7. Parameters such as the reliability of the pump over extended working periods (e.g., months), cost (below £1000), and biocompatibility (to preserve bacteria during pumping) are crucial for this application. According to this selection, only the microdispensing valve was evidenced to satisfy all the requirements. However, microdispensing valves work only in combination with an applied pressure, from an additional pumping system, into their inlet. Purchasing an external pump, defined in Table 7, was not taken in consideration as it would have raised the predefined overall cost over the limit (£2000). Therefore, it was decided to build a prototype of the additional pumping systems required for the correct functioning of the microdispensing valve.

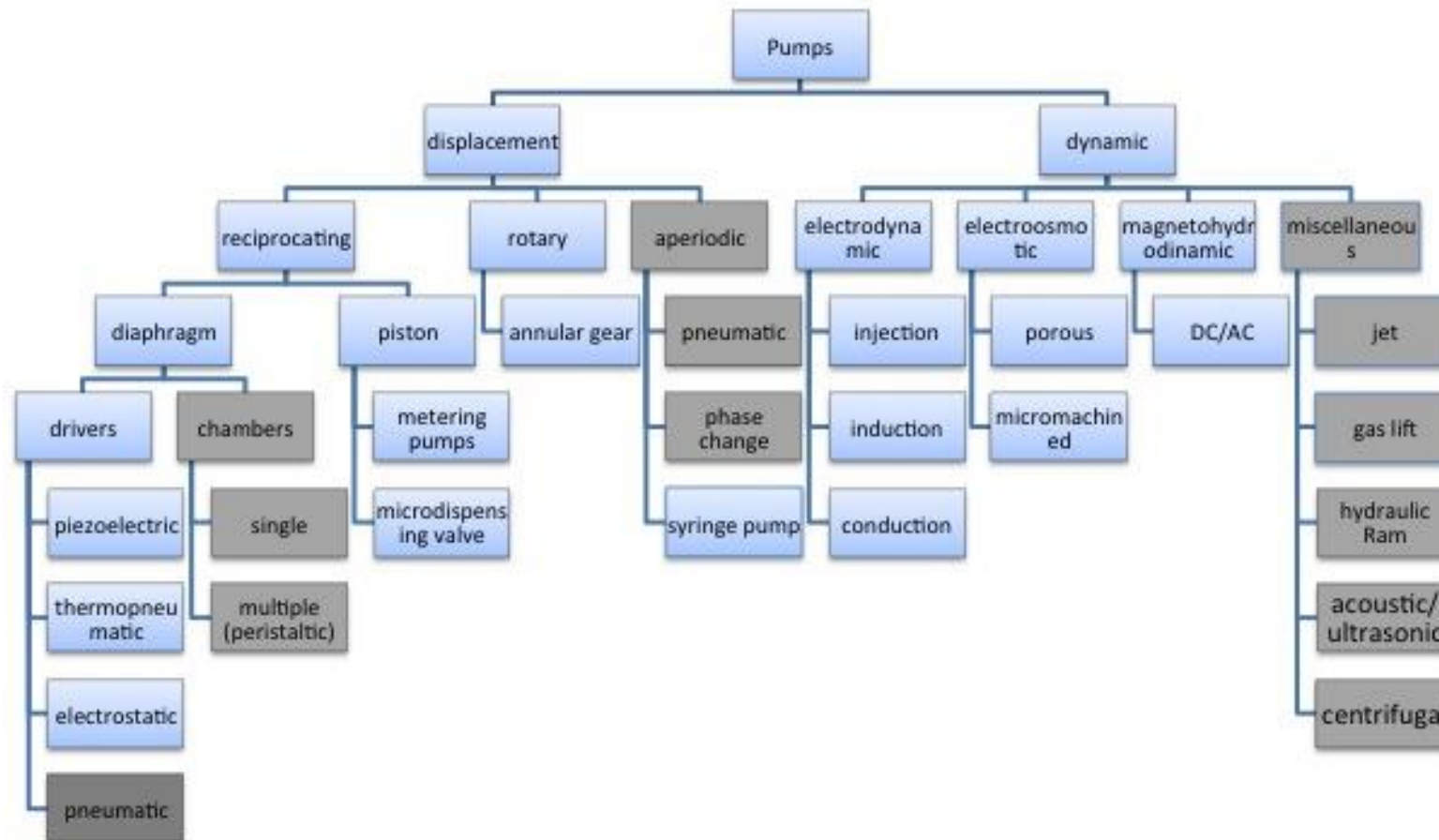


Figure 6: Classification of the pumps: non-shadowed pumps are reviewed in Table 7. Classification is reproduced from Laser & Santiago 2004.

Table 6: General classification of pumping mechanisms in microfluidics as function of the maximum back pressure and minimum volumetric fluid flow. Specifically, EHD pumps, MHD pums, piezoelectric pumps, electrostatic pumps, micromachined EO pumps, thermopneumatic pumps, pressure gas pumps, syringe pumps, annular gear pumps, peristaltic pumps, microdispensing valves, porous EO pumps and metering pump are classified in the table. Accordingly to the table, dynamic pumps such as EHD, MHD, and EO pumps may not be applied due the limitation on working liquid. Instead, the correct flow rate may be generated by pressure gas pumping systems, syringe pumps, microdispensing pumps, metering pumps, and annular gear pumps.

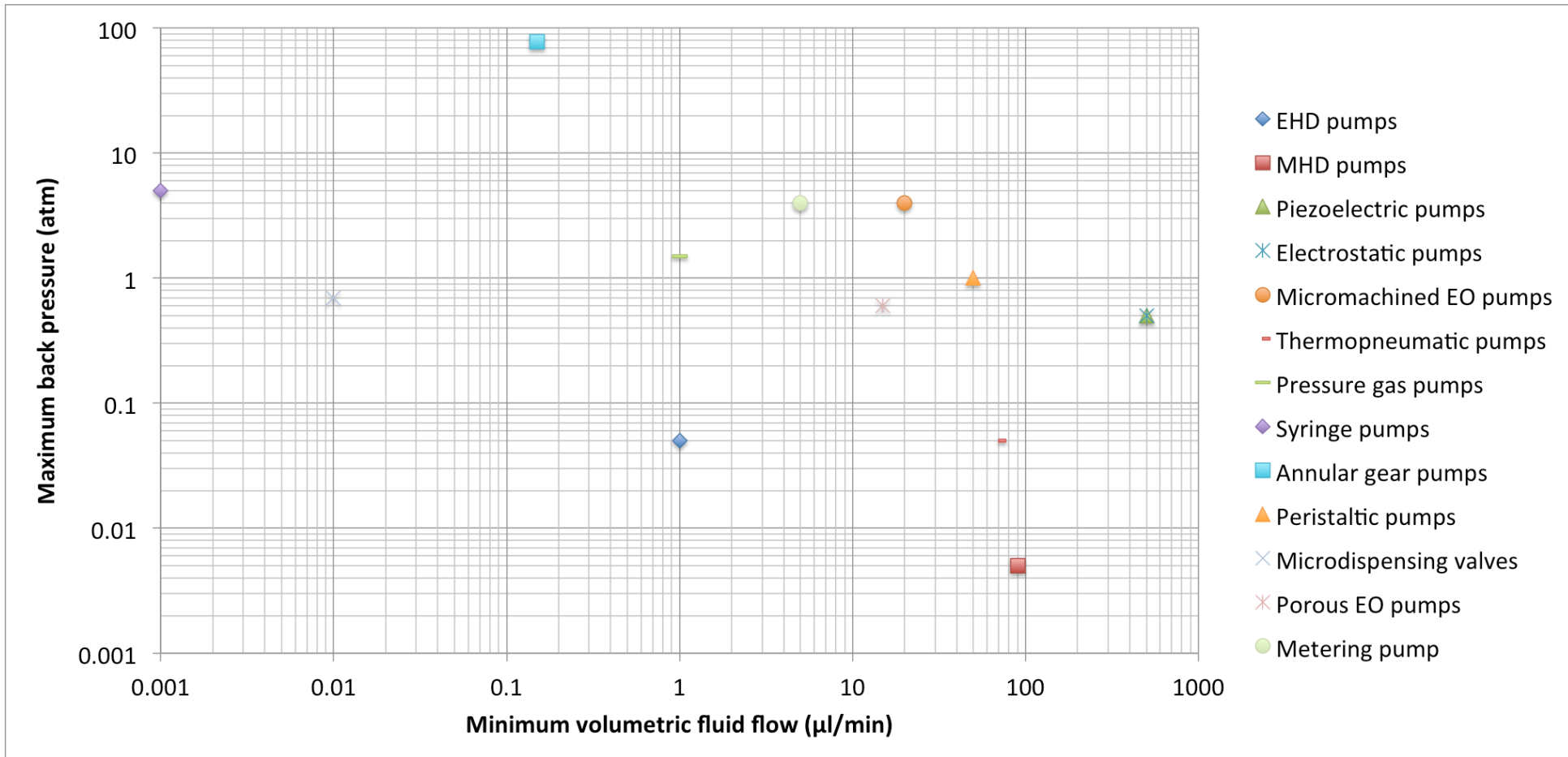


Table 7: Selection of pumping systems: in particular, annular gear pumps, microdispensing valves, pressure gas pumps and syringe pumps are able to produce a continuous flow with almost absence of pulsation. Due the cost and characteristics, only microdispensing valves are appropriate for this application. However, a microdispensing valve works only in combination with an applied pressure into its inlet from an additional external pumping system.

Pump type	Cost	Flow-rate	Wetted materials	Repeatability	Mode	Particles allowance	Priming
Annular gear pumps http://www.micropump.com/	~1600£	0.0015 – 288ml/min	Steel, ceramics, Ni-based materials, PTFE, epoxy resin	1 (%)	Continuous, pulsation 1.5%	/	Self
Metering pumps http://www.takasago-fluidics.com/	~90£	5 – 50µl/shot @ 1-4Hz	PTFE, FPM	+ - 2%	Pulse	/	Self
Syringe pumps http://www.syringepump.com/	~1500£	1nl	Glass or plastic				
Microdispensing valves http://www.theleecoefs.com/	~140£	Works with an applied pressure. The valve opens and closes continuously to control	PTFE, Elastomer	/	/	<50µm	/

		the fluid flow					
Pressure gas pumps http://www.fluigent.com/	~1900£	16 fluidic combinations, 0-7µl/min up to 1ml/min	The liquid is only in contact with the pressurized gas	0.05% Pulseless flow	Continuous	Yes	Self

2.4 ACTIVE MICROFLUIDICS ON NANOTOX, PART

II

Accordingly with the conclusion provided in the previous paragraph, an experiment was performed to evaluate the stability of a simple and inexpensive pumping system based on the combination of an aquarium air pump in series with a glass container and a fluid flow restrictor.

The set up of the equipment is illustrated in Figure 7; specification of the set up is provided in Table 8. During the experiment, a glass container was set up with 3 apertures: two outlets, one on the bottom and one on the top, and one inlet on the top of the container. The bottom outlet aperture was connected to a flow restrictor ending in a vessel, the top outlet to a pressure sensor to sense pressure variation, and the top inlet to a valve in series with a gas pump. All connections were airtight to avoid any potential decrease of pressure during the experiment.

The glass container used during the experiment was a dropping funnel, made of borosilicate glass, with nominal capacity of 500ml and a stopcock bore of 4mm. The upper entrance of the glass container was closed with a plastic airtight stopper. The stopper comprised two apertures for the top outlet and inlet as described above.

The flow restrictor was a FEP tubing of 15cm in length, 1/16 inches external diameter (OD) and 0.005 inches internal diameter (ID). The flow restrictor was connected from one side to the lower entrance of the glass container and from the other side to a plastic tubing ending in a vessel. Changes of the liquid weight of the vessel were measured and recorded during the course of the experiment.

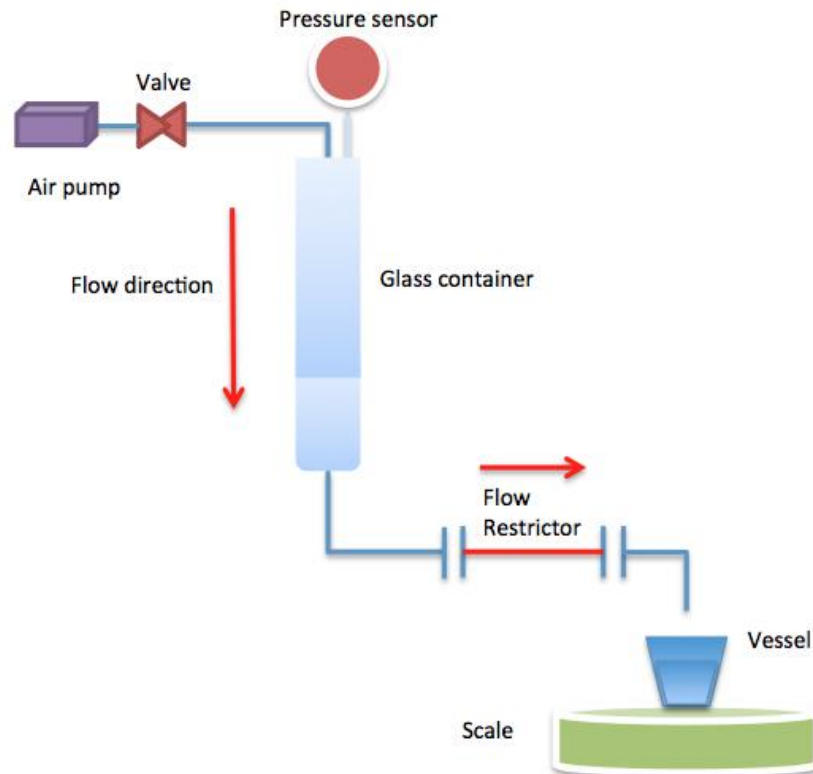


Figure 7: Set up of the equipment for gas pressure pumping; the aquarium air pump (TETRATEC APS 50) was connected to a dual stage regulator. According to the measured value with the pressure sensor (RS - DP2-42E), a static pressure (2 Bar) was obtained. The pressure generated was able to push the liquid through the flow restrictor; an FEP tubing with 1/16 inch OD, 0.005 inch ID, and 15cm in length; into a plastic vessel. Variations of the weight of the liquid were monitored over a period of 90hrs. Measurements were taken at intervals of 1 second.

Table 8: Equipment gas pressure pump

Description	Code	Company	Specification
Aquarium air pump	Tetratec APS 50	Tetratec	
Air tubing	-	-	General food grade tubing
Pressure sensor	DP2-42E	RS	0 to 1.000 MPa
Glass container	Z304379-1EA	Sigma aldrich	QUICKFIT dropping funnel, nominal capacity 500ml, and stopcock bore of 4mm
Modified cap	-	-	Customized stopper for air tube
Fluid flow restrictor	1475-20	Kinesis	FEP tubing: 1/16 inches OD, 0.005 inches ID, length: 15cm
Scale	SPU123	Ohaus	120g err 0.001g Data output in Labview via RS232
Plastic Vessel	-	-	Nominal capacity 50ml Covered with Nescofilm to avoid evaporation

Initially, 400ml of coloured water (coloured with an artificial red cochineal food colour) was poured into the glass container. Room temperature and weight of the empty vessel were recorded. Then, the glass container was closed and the air pump was activated to generate the necessary pressure to move the liquid through the fluid flow restrictor into the empty vessel. The pressure sensor readings were recorded stable at 2 Bar. The variations of the weight of

the liquid into the vessel were monitored over two consecutive periods of 90hours and 60hours. Measurements were taken at intervals of 1sec with Labview active data logging. Graph results of the experiment are shown in Figure 9, Figure 10, and Figure 8.

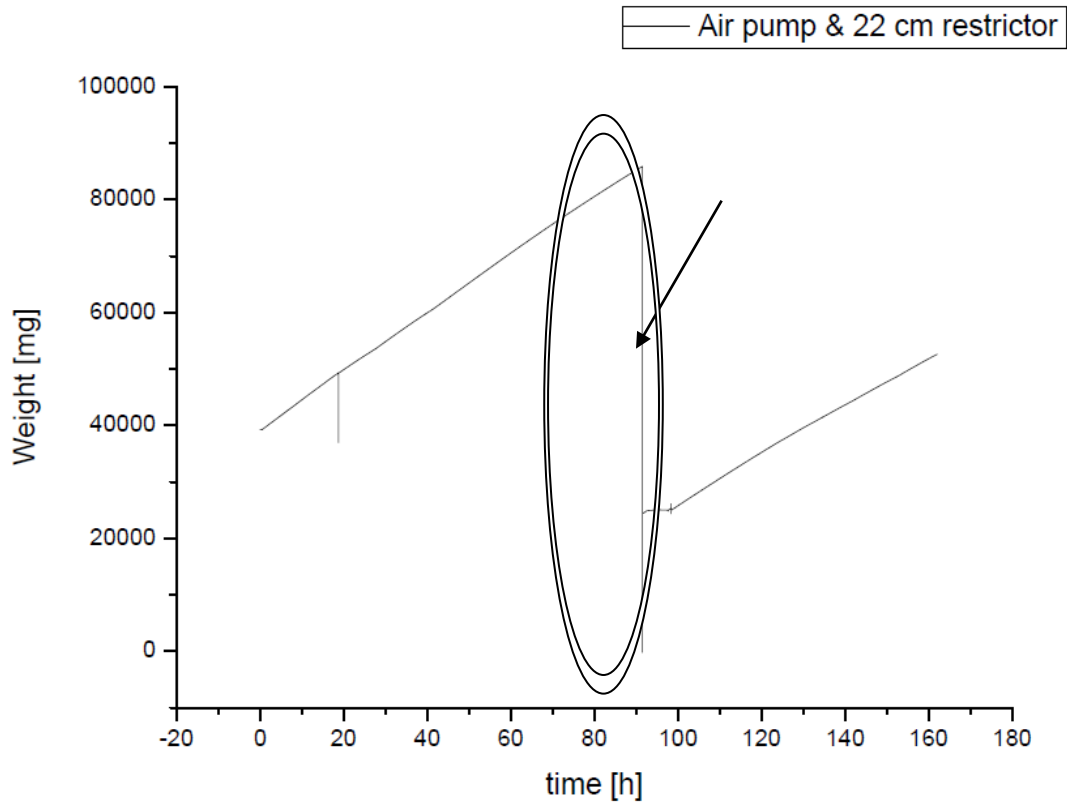


Figure 8: Graph of air pump with 22cm flow restrictor: two measurements were taken during the experiment. The first measurement was taken from 0 to 90hrs (Figure 9), and the second measurement from 100 to 160hrs (Figure 10). Vessel was manually emptied as marked in the graph (see black arrow and circle) to allow two consecutive measurements. Data were recorded for a total period of approximately 150hrs.

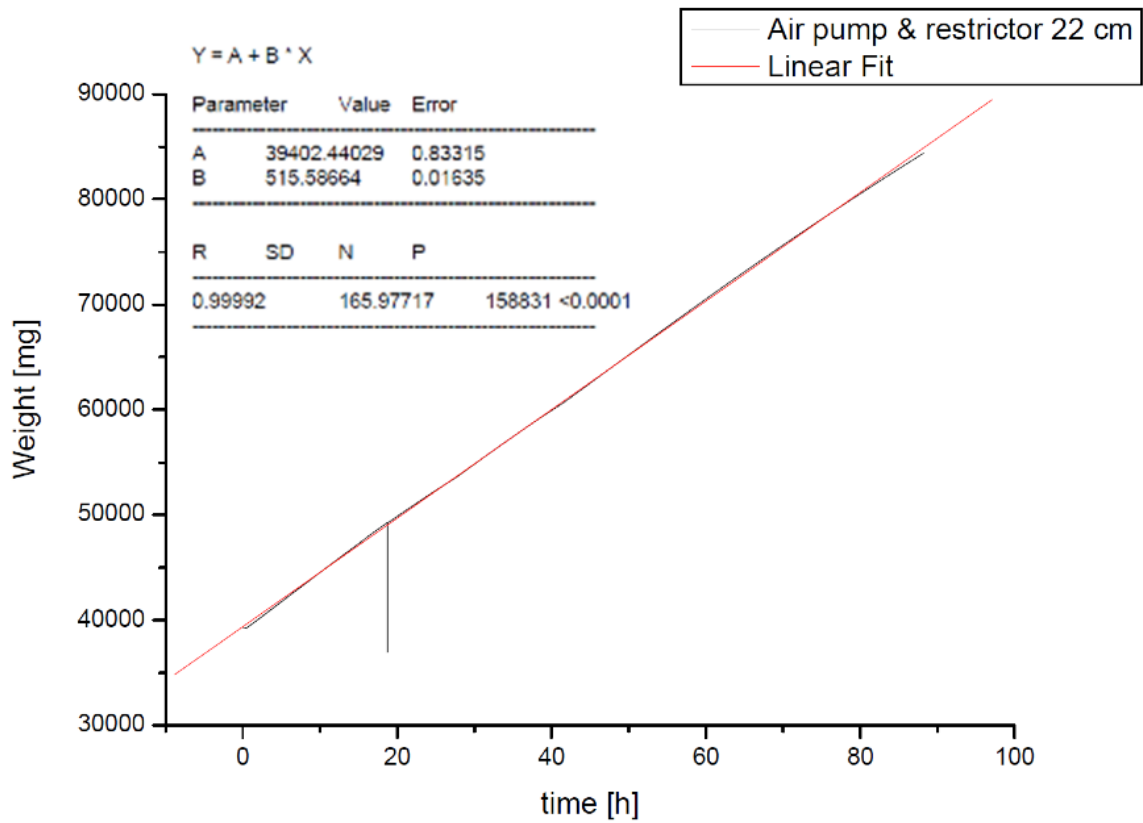


Figure 9: Air pump with 22cm flow restrictor (excerpt of graph in Figure 8 from 0 to 90hrs). Fluid flow (black curve) is almost stable; strong correlation has been observed and data stay close to the line of best fit (in red) ($R=0.99992 > R^2=0.99984$). Measurements were recorded for a period of approximately 90hrs at intervals of 1sec. After this period, the vessel was manually emptied to allow a second measurement. In particular, the spike in the black curve at approximately 20h is a data logging error.

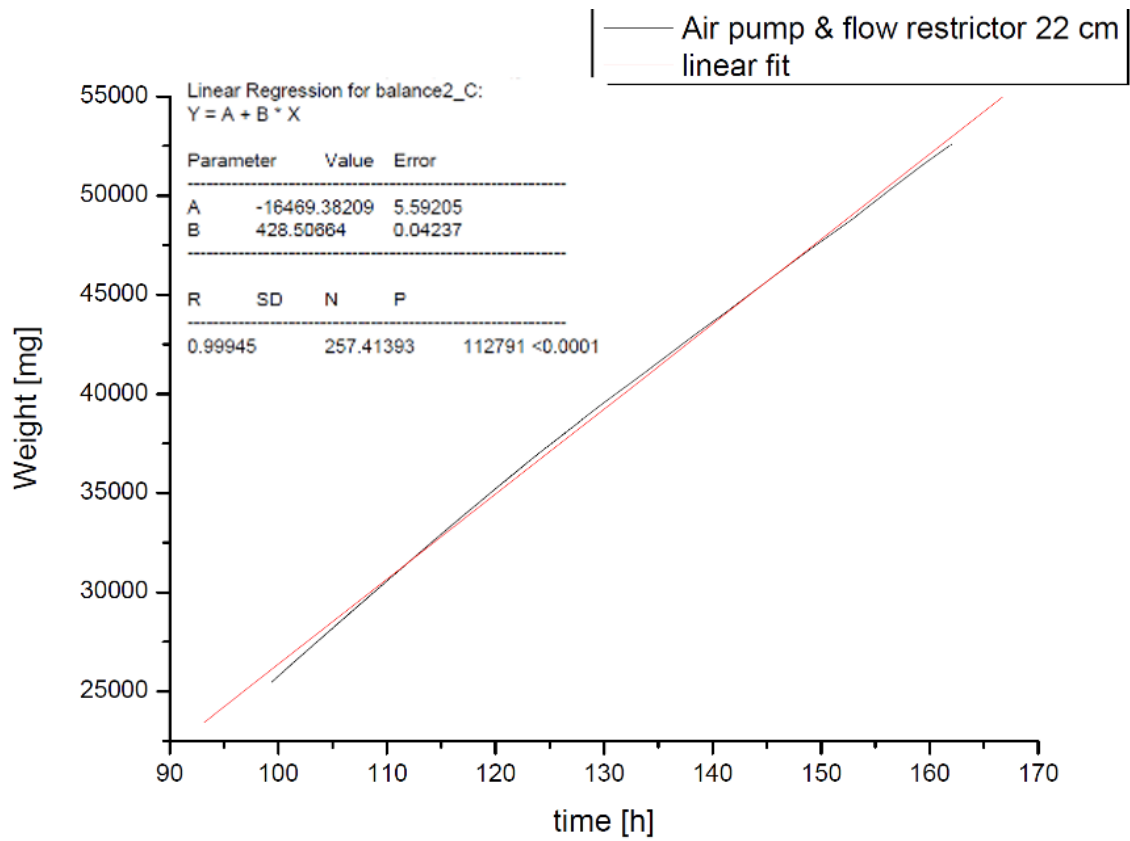


Figure 10: Air pump with 22cm flow restrictor (excerpt of graph in Figure 8 from 100 to 160hrs after vessel unloading): Fluid flow (black curve) is almost stable. Strong correlation has been observed and data stay close to the line of best fit (in red) ($R=0.99945 > R^2=0.9989$). Measurements were recorded for a period of approximately 60hrs at intervals of 1sec. Before this reading, the vessel was manually emptied.

2.4.1. CONCLUSION

The pressure sensor measured a constant value of 2.0 Bar. Pressure of the glass container was considered stable during the experiment. Measurements of the variation of the weight over time showed a strong correlation with the linear regression curve representing the line of best fit. This indicated that the prototype pumping system had produced an almost constant fluid flow over a period of 150hrs.

However, as shown in Table 9, the presence of a slight decrease of the fluid flow rate over the duration of the experiment was a clear indication that a controlling system and/or a configuration less dependent of the weight of the liquid into the glass container are necessary to reduce the decrease of the fluid flow over time (Kirby 2009). In this specific experiment, the total drop in flow rate is estimated as follow: $[(9.22\mu\text{l}/\text{min} - 6.91 \mu\text{l}/\text{min})/(9.22 \mu\text{l}/\text{min}) * 100] = 25.0542\%$.

Therefore, this prototype may be further improved by adding a control system (e.g., feedback or feedforward electronic system) and by placing the outlet of the glass container on the top so to reduce influence of gravity. Moreover, an additional microdispensing valve may be added in series with the flow restrictor (i.e. Lee microdispensing valve). The microdispensing valve may be interconnected to an electronic feedback or feedforward system to improve control over the dispensed fluid flow.

Figure 11 shows a schematic of the system comprising the aforementioned variations in the specific case in which a feedforward system is included. Also, keeping the fluidics above the mass of the fluid reservoir is needed to ensure that the mass of the fluid has no influence.

Table 9: Probed values and fluid flow rates: in particular, a decrease of 2.31 μ l/min per week has been observed. Initial fluid flow rate was 9.22 μ l/min and final flow was 6.91 μ l/min. Total drop in flow rate $[(9.22\mu\text{l}/\text{min} - 6.91\mu\text{l}/\text{min}) / (9.22\mu\text{l}/\text{min}) * 100] = 25.0542\%$.

ID Reading	Starting time (h1) [hrs]	Ending time (h2) [hrs]	Fluid flow rate [μ l/min] = weight[h2]-weight[h1]/(h2-h1)
01	1.9569	6.02	9.22
02	14.76	17.34	9.08
03	32.64	39.4	8.44
04	48.14	60.85	8.84
05	70.18	74.55	8.22
06	79.32	84.68	7.91
07	100.23	104.45	8.09
08	112.03	116.89	7.18
09	120.19	123.38	7.43
10	129.55	133.53	6.77
11	140.64	144.59	7.15
12	151.45	155.85	6.91

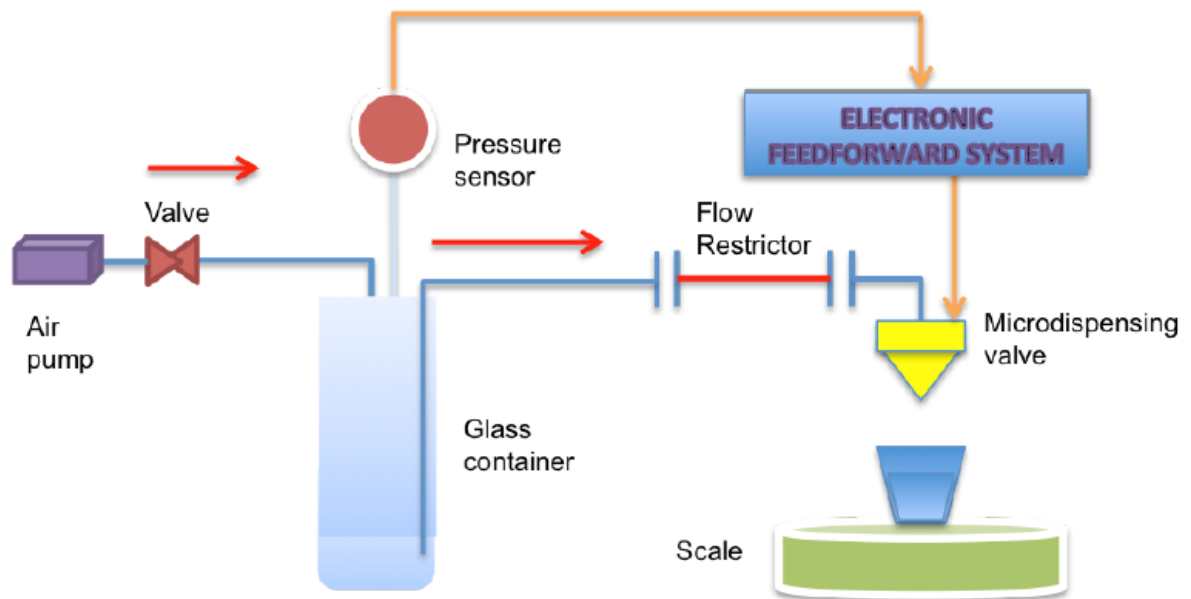


Figure 11: Schematic of the configuration with microdispensing valve and the electronic feedforward system: the aquarium air pump (TETRATEC APS 50) is connected to a glass container via a valve. The pressure sensor (RS DP2-42E) is used to check the stability of the gas pump. Pressure readings are communicated to an electronic feedforward system. The pressure generated in the glass container will push the liquid through the flow restrictor (a FEP tubing 1/16inch OD, 0.005inch ID, and 15cm in length) into a microdispensing valve, via a probing tubing placed at the top part of the glass container to reduce the variation of the fluid flow caused by the influence of the gravity. The electronic feedforward uses data from a pressure sensor to control the fluid flow into the vessel. Optionally, the electronic feedforward system may acquire data from the scale to control the microdispensing valve.

2.5 CHILLED *VIBRIO FISCHERI* IN SUBSTITUTION FOR A CONTINUOUS MICROBIAL CULTURE.

One of the most critical components is the bioreactor. If bacteria are not kept inside ideal conditions the analyser will not be able to function properly and may require a change of consumables (e.g., new microbial culture, nutrient, etc.), at a significant cost (Randles & Gray 2012).

The introduction of an alternative system that preserves bacteria over extended periods of time, at least one month (average life expectancy of a new culture), will have the advantage of removing the presence of the bioreactor, reducing the need for complicated pump control systems for bioreagent maintenance, gaining simplicity, and reducing the overall cost of the analyser. An example of the schematic introducing chilled bioreagent is shown in Figure 12.

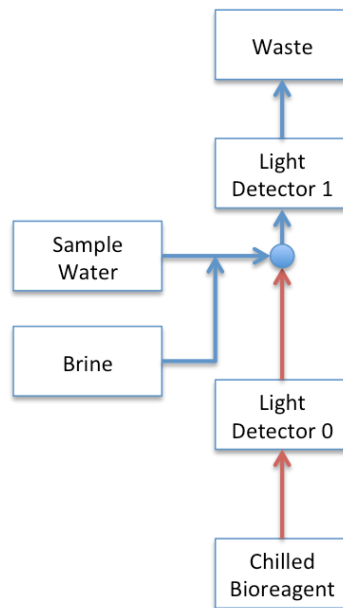


Figure 12: Improved schematic of NANOTOX: the device continuously harvests bioluminescent bacteria (chilled bioreagent) from a reservoir, mixes them with sample water and brine (buffer). NANOTOX measures changes of light of the bioreagent after the interaction with the sample water, and allows automatic, real-time detection of contaminants in water. The chilled bacteria reservoir is applied in substitution of the microbial bioreactor and the microbial culture medium (Nutrient). It is aerated, stirred and temperature controlled to maintain the bacteria under chilling condition. Light output is measured using photomultiplier tubes (PMTs). Tubings representing the red line in picture might inhibit any contamination from flowing back into the reservoir.

Schematic of the configuration with chilled *Vibrio fischeri* in substitution of a continuous microbial culture is represented in Figure 13. The bioreagent may be usually preserved for at least a month under chilling conditions in a glass container. It may be pushed out of the glass container by applying a constant pressure. The interaction of bioreagent with the sample water can take place at the mixing node. The photodetectors PMT (L_1) and PMT (L_2) detect the light changes of the bioreagent after it gets in contact with the sample water. Light detector PMT (L_0) provides status of health of raw bioreagent when warms up to ambient temperature (22 °C).

As provided in the earlier discussion of the CTM system in Figure 4 and similarly here in Figure 13, blank solution, not shown in this schematic for simplicity, is used to obtain a first response, a baseline L_B , from light detector PMT (L_1) and thus calibrate the system to further establish quality of the sample water by comparing the L_B to L_1 output. On the other hand, light detector PMT (L_0) provides status of health of raw bioreagent from the fermentor, prior to interaction with sample water at mixing node.

Equally to the CTM, in this example in Figure 13, PMT (L_2) provides a response at 5min after bioreagent interaction with sample water.

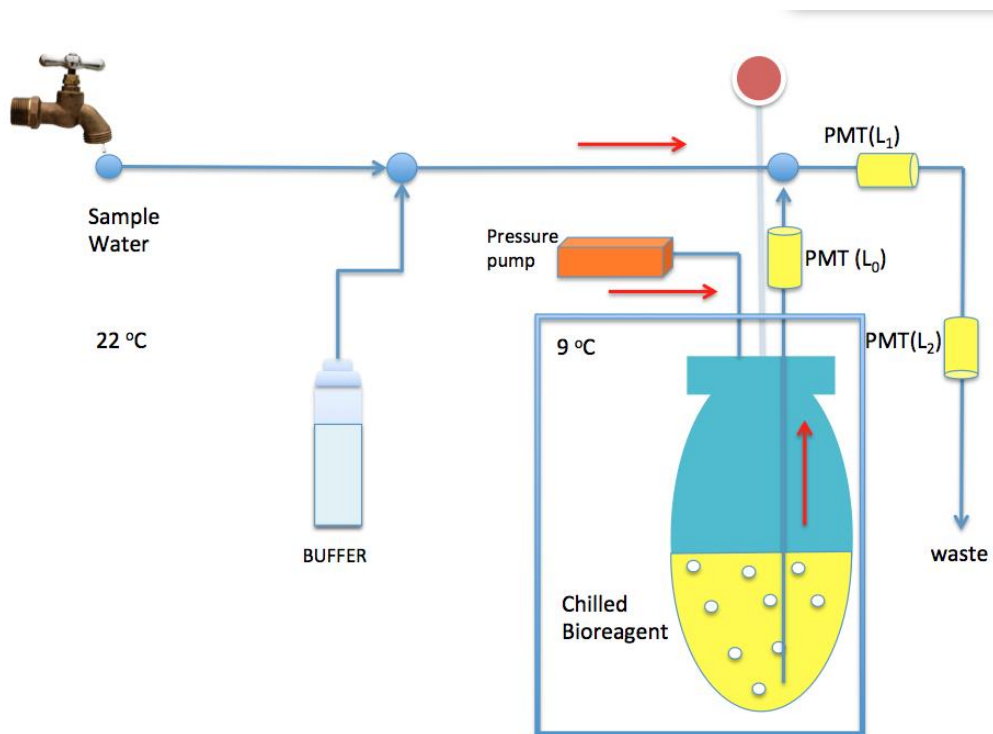


Figure 13: Description of the main working mechanism with chilled bioreagent: two regions are set at different temperatures to control biofilm formation and preserve the microbial culture for long time storage. The first region will be cooled by means of a thermoelectric couple at around 9 °C, this region will include the bioreagent reservoir and a fluid flow restrictor. All the other regions might be set at 22 °C to activate bacteria bioluminescence. Chilled bacteria in yellow are pushed out from a pressurized reservoir in a controlled way by applying a fluid flow restrictor. The light detectors detect the bioluminescence of bacteria before (PMT (L_0)) and after contact with the mixed solution (PMT (L_1)) provides a response at 2min, and PMT (L_2) provides a response at 5min).

2.5.1. EFFECT OF CHILLED BATCH MICROBIAL CULTURE OF *VIBRIO*

FISCHERI IN SUBSTITUTION FOR A CONTINUOUS MICROBIAL CULTURE AND INTERACTION WITH $ZnSO_4$

Two experiments were performed to appraise the effect of a chilled batch of microbial culture in substitution for a continuous microbial culture, and to estimate whether the chilled bacteria may provide bioluminescence readings comparable to readings obtained with continuous microbial culture.

During a first experiment, the applied temperature changes at the water bath induced a response from the bioreagent line. The experiment started by preparing duplicate conical flasks (50ml) containing M18 microbial culture medium (150ml). The flasks were autoclaved at a temperature of 121°C for 20 minutes and allowed to cool before inoculation. The flasks were inoculated with dried frozen *Vibrio fischeri* (NRL 11177). The microbial cultures were incubated in a reciprocating shaker (Gallenkamp) at ambient temperature (~22°C), shaking at 80 rpm for 24-48 hrs. The flasks were removed from the incubator once the bioreagent was visibly observable and stored in the fridge for 2 days at 9 °C. The microbial culture from the duplicate flasks was poured into a 500ml Duran glass, which was fitted in a wine cooler. The cooler was set at 9 °C to maintain bacteria under chilled conditions. A thermometer was inserted into the microbial culture, in the wine cooler, for the entire duration of the experiment, to record the temperature changes of the microbial culture. A silicone tube (1.5mm ID, wall 0.5mm) was used to collect bioreagent from the Duran glass. This tube was connected to another silicone tube; the latter was used as pump tube for bioreagent. An approximate length of 15cm of the former silicone tube was immersed into a Grant water bath set firstly at 27°C and successively, as show in Figure 15, to 35°C. This was done to set the temperature of the chilled bioreagent at 22°C before getting in proximity of PMT (L_0).

A concentration of 10% NaCl, based on volume, in water (brine) was pumped through the brine pump; distilled water was used as sample water. The sample was mixed with the brine to obtain a final concentration of 1% brine. The mixed solution was then mixed with the bioreagent, and the resulting was passed through a tubing. The photon emission of the mixed solution was detected with PMT (L_1) and PMT (L_2) (Hamamatsu, H5784) at $T = 2$ minutes and $T = 5$ minutes after the mixing point. The PMTs were positioned in individual black capsules which do not allow the tubing to slip and significantly reduce external light contamination. The photon emission of the raw bioreagent was detected with PMT (L_0).

Set up is presented in the **Figure 14** according with the above description.

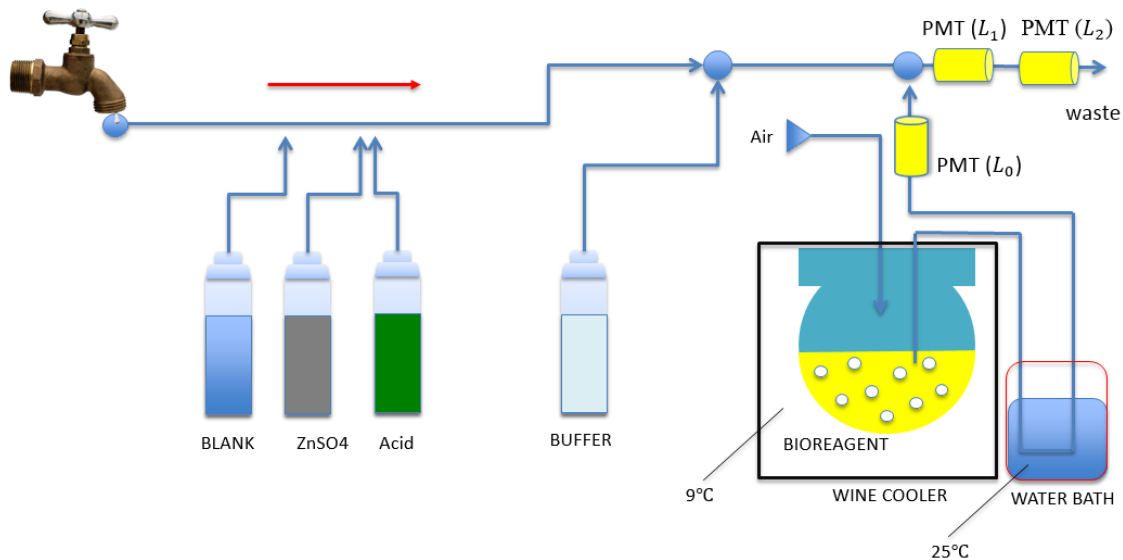


Figure 14: Schematic of the Continuous Toxicity Monitor (CTM) readapted for experiments with chilled bioreagent: during the performed experiment, the CTM continuously harvests bioluminescent bacteria (bioreagent) from a chilled bioreagent (bioreagent) fitted in a wine cooler (wine cooler), mixes them with sample water (distilled water) and brine (buffer) to dilute the bioreagent and allow reaction. Bioreagent is aerated, stirred, wine cooler temperature maintained to 9°C . Water bath was set initially at 27°C and successively at 35°C to set reagent at $\sim 22^{\circ}\text{C}$ to allow detection. Light output is measured using photomultiplier tubes (PMTs), 2 and 5 minutes after mixing point. The reagent section comprises a vessel with distilled water (BLANK) used to set a baseline light output from which inhibition may be evaluated. A calibrant solution (zinc sulphate (ZnSO_4)) was used in these experiments to perform two standard toxicity tests with known concentration (10ppm ZnSO_4). Cleaning reagent, such as citric acid (Acid) is used for daily cleaning procedure. The waste section comprises a waste tank.

In a second experiment, the interaction of the bioreagent with ZnSO₄ was studied. In this case the set-up of the first experiment was repeated accordingly with the above description as also presented in **Figure 14** above.

A concentration of 10% NaCl, based on volume, in water (brine) was pumped through the brine pump. The sample was mixed with the brine to obtain a final concentration of 1% brine. At 9:30 in **Figure 14** distilled water with 2.5 mg/L of ZnSO₄ was introduced in substitution to the above sample water.

The mixed solution was then mixed with the bioreagent, and the resulting final solution was passed through a tubing. The photon emission of the mixed final solution was detected by PMT (L₁) and PMT (L₂) (Hamamatsu, H5784) at T = 2 minutes and T= 5 minutes after the mixing point. The photon emission of the raw bioreagent was detected with PMT (L₀).

It is worth to note that in all experiments the same PMT model set with same conditions are used for all the PMTs of the CTM. The only difference between the various PMTs is the location of detection.

Details of the pumps and tubes are shown in Table 10.

Table 10: Details of pumps and tubing

<u>Bioreagent pump and tubing</u>
<ul style="list-style-type: none"> • Bioreagent flow rate: Target= 0.18ml/min, measured flow rate: 0.19ml/min • Bioreagent pump tubing: AlteSil high strength silicone tubing from ALTEC, 1mm x 1mm. Lot no: 2277602 • Bioreagent pump: peristaltic pump (pump set at a calibration value of 04.20rpm)
<u>Methods: Brine pump and tubing</u>
<ul style="list-style-type: none"> • Brine flow rate: Target = 0.24ml/min, measured flow rate: 0.24ml/min • Brine pump tubing: AlteSil high strength silicone tubing from ALTEC, 1mm x 1mm,

Lot no: 2277602

- Brine pump: peristaltic pump (pump set at 03.80rpm)

Methods: Sample pump and tubing

- Sample flow rate: Target = 2.84ml/min
- Sample pump tubing: MASTER FLEX 06404-14 Neoprene, 2mm x 2mm, Mfg by Saint – Gobain
- Sample pump: peristaltic pump calibration value set at 28.00
- Sample pump: pump YZ1515x with three metal rollers. The sample pump is currently in the pull position, after the bioreagent-sample mixing point
- The flow rate of the waste sample was measured to be 2.99ml/min

Methods: Residence time coil tubing

The residence time loops (to include in front of PMT) used 1.5mm ID platinum cured stock tube (Supplier Silex; product code NGP 60 T (cure date: 16/02/09, batch no: 546664), wall 0.5mm)

2.5.2. RESULTS AND CONCLUSIONS

As results, graphs are provided herein, as in Figure 15 and in Figure 16, indicating PMTs' readings. Specifically, PMT (L_0) readings (i.e. raw bioreagent) are higher than PMT (L_1) readings (i.e. mixed solution after 2 minutes) and the PMT (L_2) readings (i.e. mixed solution after 5 minutes).

The readings confirm that the bioreagent reacts successfully when in contact with the sample water, such as distilled water (e.g., PMT (L_1) reading in Figure 15), and distilled water with 2.5 mg/L of ZnSO₄ (e.g., PMT (L_1) reading in Figure 16).

Notably spikes may be observed in Figure 17 for both the PMT (L_1) and the PMT (L_2) readings. Spikes precede drop in photon counts indicating an inhibitory effect of ZnSO₄ to the chilled batch. This effect was also noted in previous recording of CTM. Although no further studies were performed in this project to understand this phenomena, there appear that spikes may be associated to an initial reaction of the bacteria when in presence of an external agent within the water sample.

Further, Figure 16 shows the Inhibitory effect of ZnSO₄ (2.5 mg/L) on the chilled batch microbial culture of *Vibrio fischeri* in substitution with a continuous microbial culture. Percentage of the inhibitory effect was 95% at PMT (L_1) and 98% at PMT (L_2) (Figure 18).

This was an excellent response similar to the response with continuous microbial culture, as recorded in previous experiment performed by Modern Water.

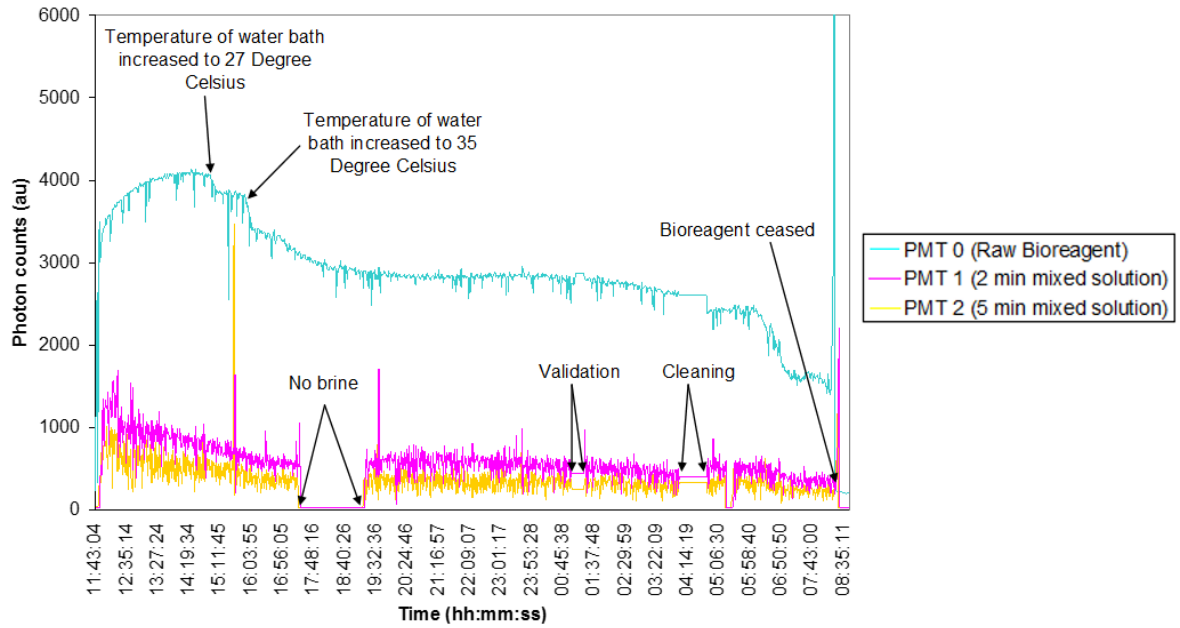


Figure 15: Photon counts of raw bioreagent and mixed solution with chilled bacteria in substitution for a continuous microbial culture in the CTM analyser: PMT 0, PMT 1, and PMT 2 are respectively PMT (L_0), PMT (L_1), and PMT (L_2). PMT (L_0) provides raw bioreagent light reading (blue) that reflects status of bioreagent. PMT (L_1) and PMT (L_2) are respectively light readings at 2 minutes (purple) and 5 minutes (yellow) after mixing. Temperature of the water bath was changed during the experiment (from 27 °C to 35 °C). Background toxicity with distilled water was successfully detected.

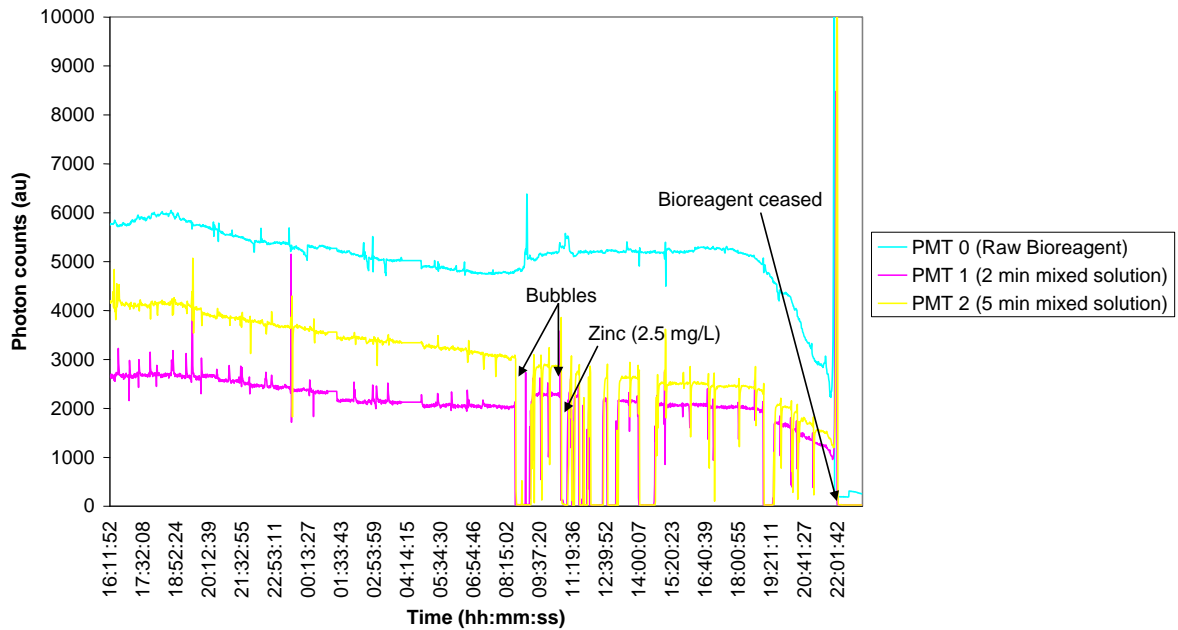


Figure 16: Photon counts of raw bioreagent and mixed solution with chilled bacteria in substitution for a continuous microbial culture in the CTM analyser. Effect of the $ZnSO_4$ is shown in the picture. PMT 0, PMT 1, and PMT 2 are respectively PMT (L_0), PMT (L_1), and PMT (L_2). PMT (L_0) provides raw bioreagent light reading (blue) that reflects status of bioreagent. PMT (L_1) and PMT (L_2) are respectively light readings at 2 minutes (purple) and 5 minutes (yellow) after mixing. Temperature of the water bath was kept constant during the experiment (35 °C). When in presence of $ZnSO_4$ (2.5 mg/L) an inhibitory effect was recorded.

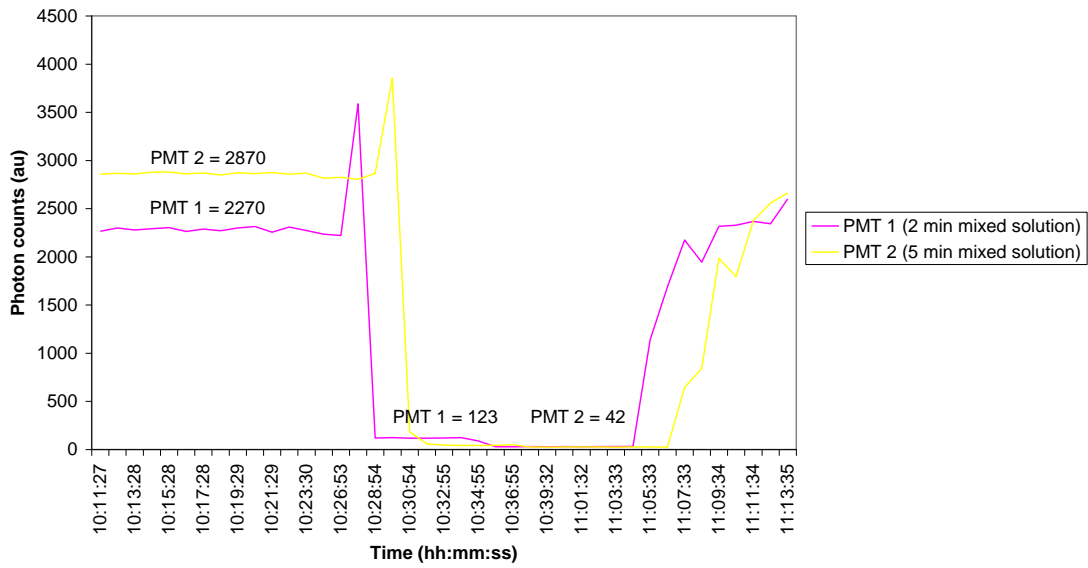


Figure 17: Effect of the ZnSO₄ (2.5 mg/L) on the chilled batch microbial culture of *Vibrio fischeri* in substitution with a continuous microbial culture in the CTM analyser: when in presence of ZnSO₄ (2.5 mg/L) an inhibitory effect was recorded. PMT 0, PMT 1, and PMT 2 are respectively PMT (L₀), PMT (L₁), and PMT (L₂). PMT (L₁) and PMT (L₂) are respectively light readings at 2 minutes (purple) and 5 minutes (yellow) after mixing.

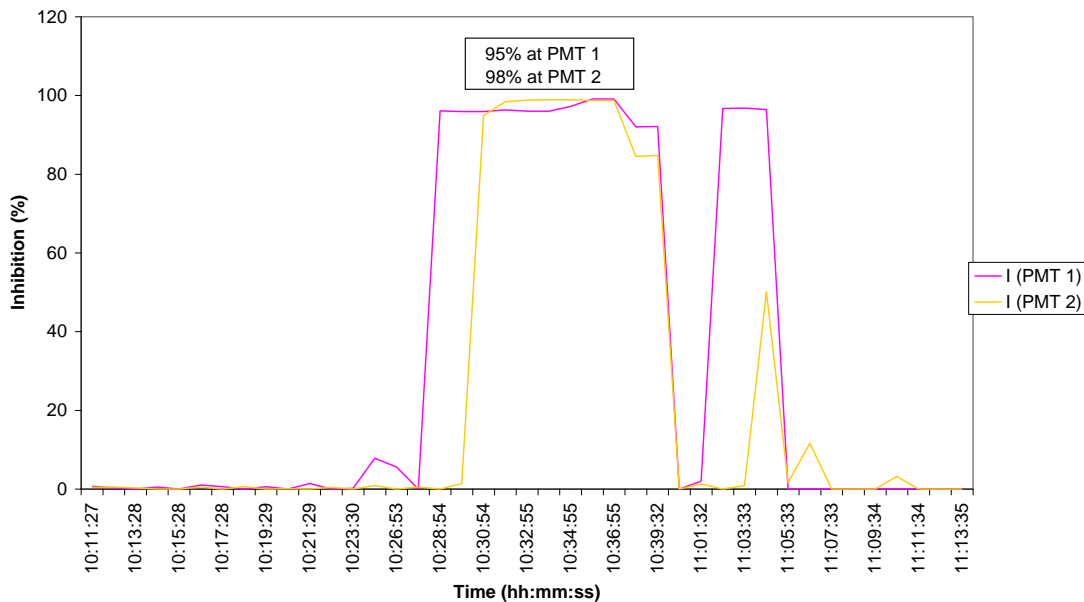


Figure 18: Percentage of inhibition with 2.5 mg/L ZnSO₄ in the CTM analyser: when in presence of ZnSO₄ (2.5 mg/L) an inhibitory effect of 95% at PMT1 and 98% at PMT2 was detected. PMT 1, and PMT 2 are respectively PMT (L₁), and PMT (L₂). PMT (L₁) and PMT (L₂) are respectively light readings at 2 minutes (purple) and 5 minutes (yellow) after mixing.

The fact that bacteria can be chilled to preserve their condition over short term period appears well known in the literature. For example, a broad range of anaerobic and aerobic bacteria may resist long-term storage by applying well-known preservation methods (Kessler & Redmann 1974), such as:

- storage with liquid paraffin;
- drying over sand and silica gel;
- drying with agar or other media;
- short term storage at +4°C;
- long term storage at -10°C to -30°C;
- freeze drying techniques;
- lyophilisation;
- storage in solid carbon dioxide; and
- preservation under liquid nitrogen.

However, there appear that none of the commercially available systems provide similar arrangement as provided in accordance with this experiments.

Modern Water undertook several experiments to determine the viability of chilled *Vibrio fischeri* diluted in a microbial culture medium and under chilling conditions over a period of few weeks. Results demonstrated that viable plate counts, periodically performed during the experiment, did not differ significantly over time. This demonstrated that storing bacteria by controlling the temperature is an effective preservation method over a period of time

proximate to one month. Therefore, chilled bacteria may be substituted to a continuous culture.

It is also important to note that every microbial culture differ to others in terms of stage of growth and viability. Accordingly, photon counts of raw bioreagent may be different for every culture. This is especially remarkable if microbial culture are in different states (e.g., chilled culture, continuous culture, etc.). In this prospect, the photon counts of the raw bioreagent of the batch microbial culture of chilled *Vibrio fischeri* differs to the photon counts of the raw bioreagent of the continuous microbial culture. This is reasonably expected as cooling bioreagent at 9°C may partly damage *Vibrio fischeri* in the culture as the bacteria are outside their ideal condition.

However, although the photon counts of the raw chilled bioreagent appears less than in a continuous culture, response to contaminants appears excellent according to the provided results. In conclusion, it was observed that the chilled *Vibrio fischeri* are viable for detection, and therefore may be used as substitution for a continuous microbial culture.

2.6 USE OF STEPPED FLOW MIXER (SFM) TO ENABLE THE REDUCTION OF THE DIFFERENTIAL PRESSURE AT MIXING NODE

Hydraulic blockage has been demonstrated to be a detrimental effect for the CTM. It is built as a consequence of the pressure generated by two fluid flows converging at the same mixing point with highly different flow rates. When the rate of the fluid flow “A” is consistently higher than the flow rate of the fluid flow “B”; the fluid flow “A”, as a consequence of a backpressure generated at the point of connection, tends to stop the fluid flow “B” (Hinman 1971; Idel’chik & Fried 1996). The use of one T-connection when mixing liquids at vastly different flow rates may lead to hydraulic blockage (Figure 19).

Hydraulic blockage may equally arise in the miniaturised CTM, NANOTOX, as consequence of the vastly different flow rates (see Table 4) at mixing node with sample water and brine and with bioreagent and salty sample water. Accordingly, a fluid blockage preventing system is necessary when mixing at large dilution. An investigation was performed to evaluate the stepped flow mixer (SFM) (Figure 20) as a method to reduce the pressure generated at the mixing node.

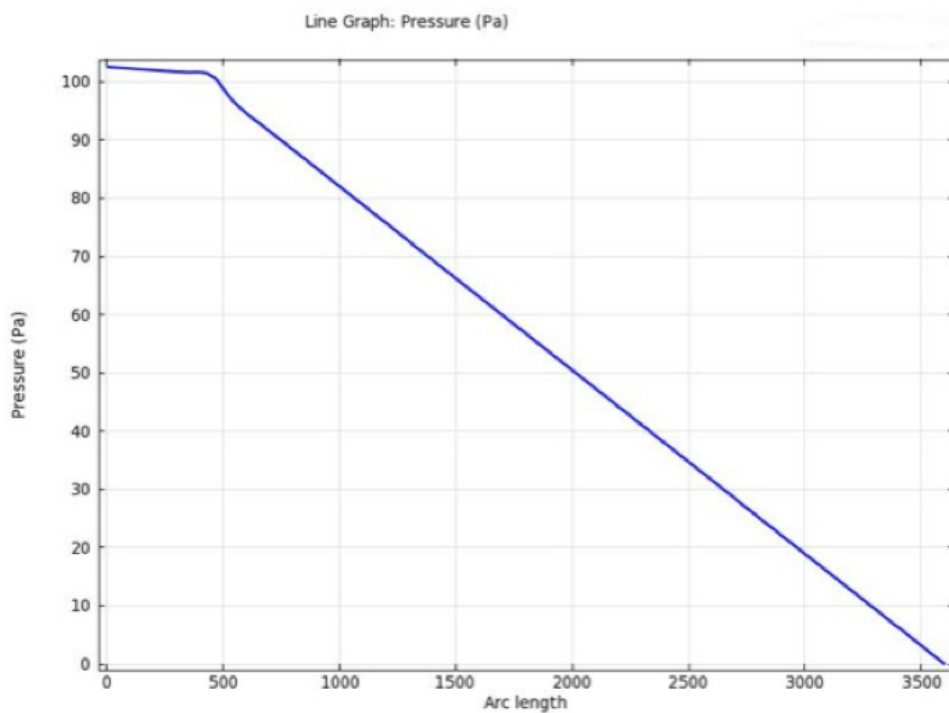
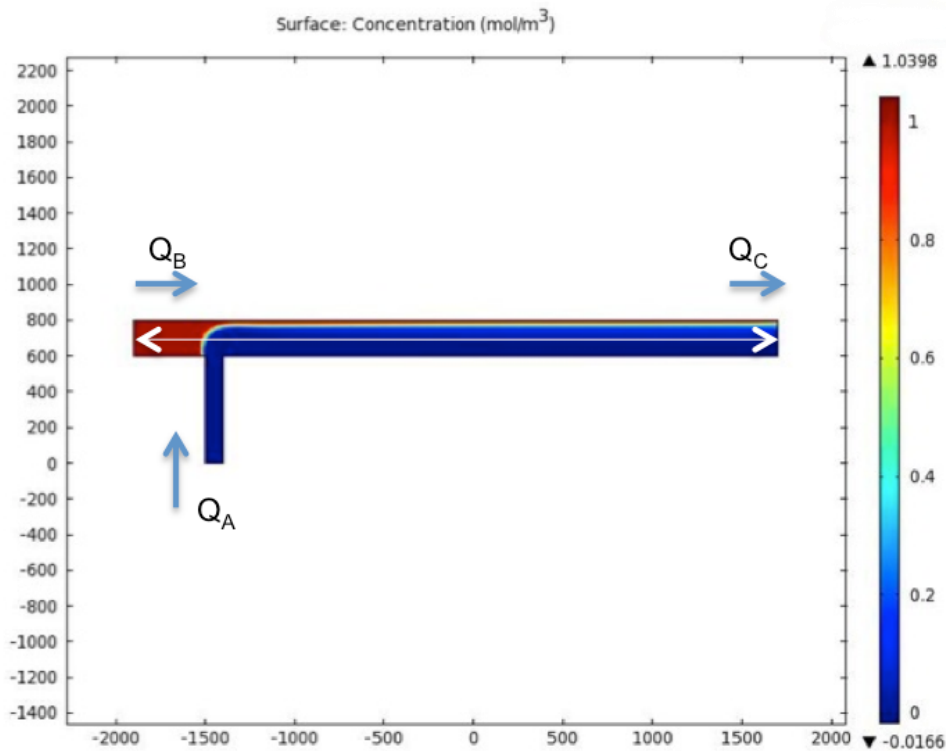


Figure 19: FEM model of a T-connection showing surface concentration of two different liquids (top) and pressure line graph along the horizontal duct (bottom). The use of a T-connection when mixing liquids at vastly different flow rates may lead to hydraulic blockage. In particular, as shown in the model (top), bioreagent (red) is compressed toward the top wall of the horizontal channel at mixing node with sample water (blue). Peak pressure (bottom graph) is equivalent to 110 Pa at the mixing node. High pressure is thus developed when vastly different volumetric fluid are applied. In this case, flow rate Q_B (red) is $7\mu\text{l}/\text{min}$ and Q_A (blue) is $70\mu\text{l}/\text{min}$.

A schematic of the stepped flow mixer (SFM) is shown in Figure 20. It consists of a tree cascaded mixer that divides the volumetric fluid flow Q_A through the branches in order to reduce the effect of the fluid flow blockage. Q_A mixes sequentially with Q_B after being divided through the branches at different flow rates ($Q_A/4$, $Q_A/4$, $Q_A/2$). The result is a sequential mixing with a distributed pressure over the mixing points.

Given an arbitrary set of branches (Q_1 , Q_2 , Q_3 , ... Q_n) the initial volumetric flow rate Q_A is split as shown in Equation 3.

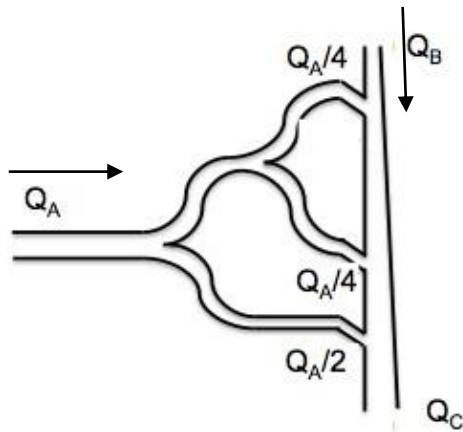


Figure 20: Cross-sectional view of the Stepped Flow Mixer (SFM): the SFM consists of a tree cascaded mixer able to divide the volumetric fluid flow Q_A through the branches in order to reduce the effect of the fluid flow blockage. Q_A mixes sequentially with Q_B , after mixing $Q_C = Q_A + Q_B$ is obtained. Flows direction are indicated by the arrows. The result is a mixing with a distributed pressure over the mixing points.

Equation 3

$$Q_A = Q_1 + Q_2 + \dots + Q_n \Rightarrow Q_A = \sum_{i=1}^n Q_i$$

$$Q_A = \frac{Q_A}{2} + \frac{Q_A}{4} + \frac{Q_A}{8} + \frac{Q_A}{8} + \dots + \frac{Q_A}{n} \Rightarrow Q_A = \left[\frac{Q_A}{2^{n-1}} + Q_A \sum_{i=2}^n \frac{1}{2^{i-1}} \right]_{n \geq 2}$$

The volumetric flow rate Q_A is equal to the cross sectional area A_A multiplied by the linear velocity v_A (Equation 4)

Equation 4

$$Q_A = A_A v_A$$

Therefore, considering the cross sectional area of the duct constant for all the branches, and equal to A_i , v_A may be obtained from Equation 3 and for $n \geq 2$ as follows (Equation 5):

Equation 5

$$v_A = v_1 + v_2 + \dots + v_n \Rightarrow v_A = \sum_{i=1}^n v_i \Rightarrow v_A = \frac{v_A}{2^{n-1}} + v_A \sum_{i=2}^n \frac{1}{2^{i-1}}$$

$$v_A = \frac{1}{2} v_A + \frac{1}{2} v_A, \quad n = 2$$

$$v_A = \frac{1}{2} v_A + \frac{1}{4} v_A + \frac{1}{4} v_A, \quad n = 3$$

For each one of the branches, the pressure (p_i) is equal to $\frac{1}{2} \rho v_i^2$. Notably, for a given flow rate Q_A variation of the cross sectional area affect the velocity and pressure in accordance with Equation 4 above.

When just one branch is used, i.e. for $n = 1$, the pressure is $p_A = \frac{1}{2} \rho v_A^2$. Accordingly, differential pressure ($p_A - p_i$) is positive (Equation 6) because $p_A < p_i$. Consequently, backpressure generated at the mixing nodes is reduced.

Equation 6

$$p_i = \frac{1}{2} \rho v_i^2 > 0$$

$$(p_A - p_i) = \frac{1}{2} \rho (v_A^2 - v_i^2) > 0$$

The SFM was simulated with COMSOL to estimate the distribution of the pressure over the mixing points in comparison of the pressure generated at the T-connection in Figure 19.

Figures 20 and 21 are exemplary SFM arrangements with respectively 3 branches ($n=3$) and 4 branches ($n=4$).

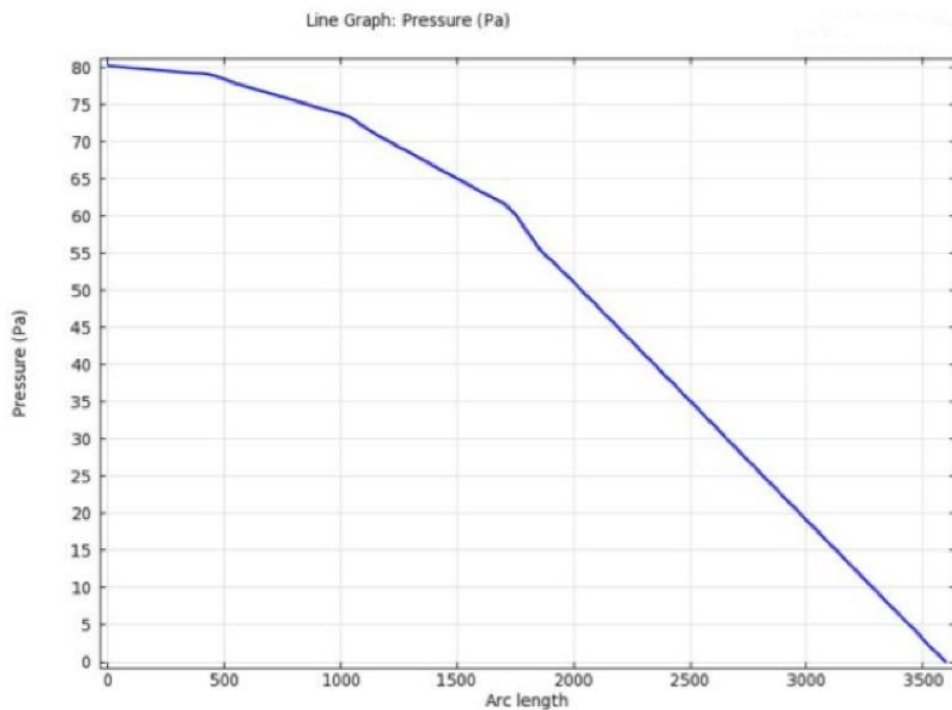
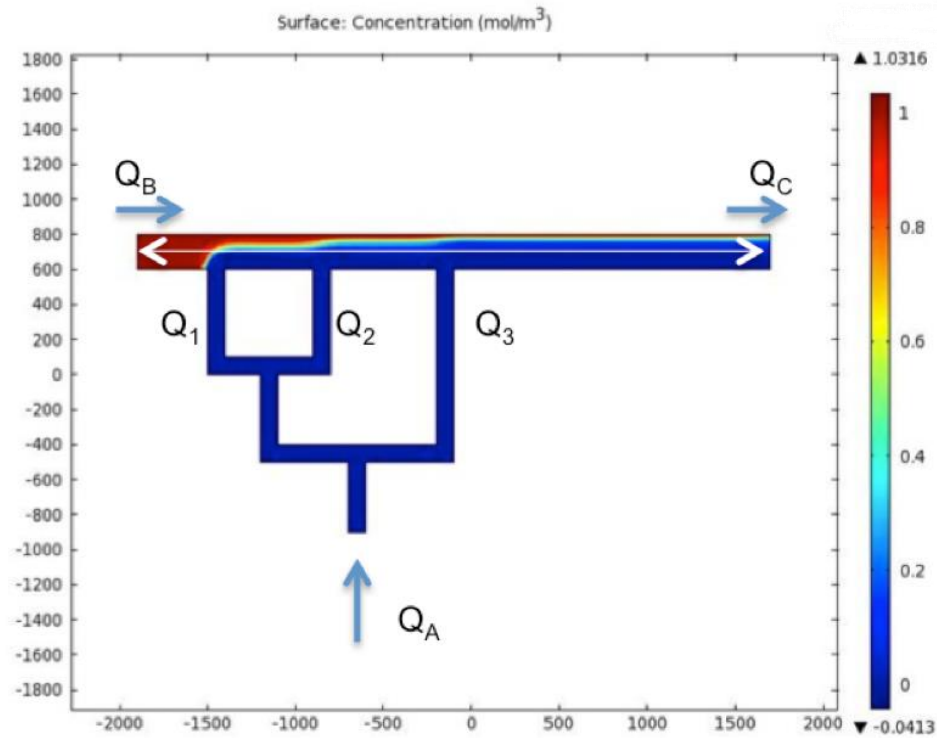


Figure 21: FEM model of SFM with three branches: use of SFM to reduce the effect of hydraulic blockage as consequence of the pressure generated at one mixing point. Surface concentration of two liquids in a SFM with three branches (top) is represented in the graph. In particular, bioreagent (red) is compressed toward the top wall of the horizontal channel when in contact with the sample water (blue) due the pressure generated at the mixing

nodes. In this specific arrangement, pressure peak is equivalent to 80 Pa (bottom): 27.28% less than the peak pressure built at the mixing node in Figure 19. Volumetric fluid flow Q_B (bioreagent) and Q_A (sample water) were set respectively at $7\mu\text{l}/\text{min}$ and $70\mu\text{l}/\text{min}$ at the two inlets. Applying a stepped-flow mixer enabled a reduction in the differential pressure between the two fluids being mixed. This enabled effective mixing while minimizing the risk of hydraulic blockage.

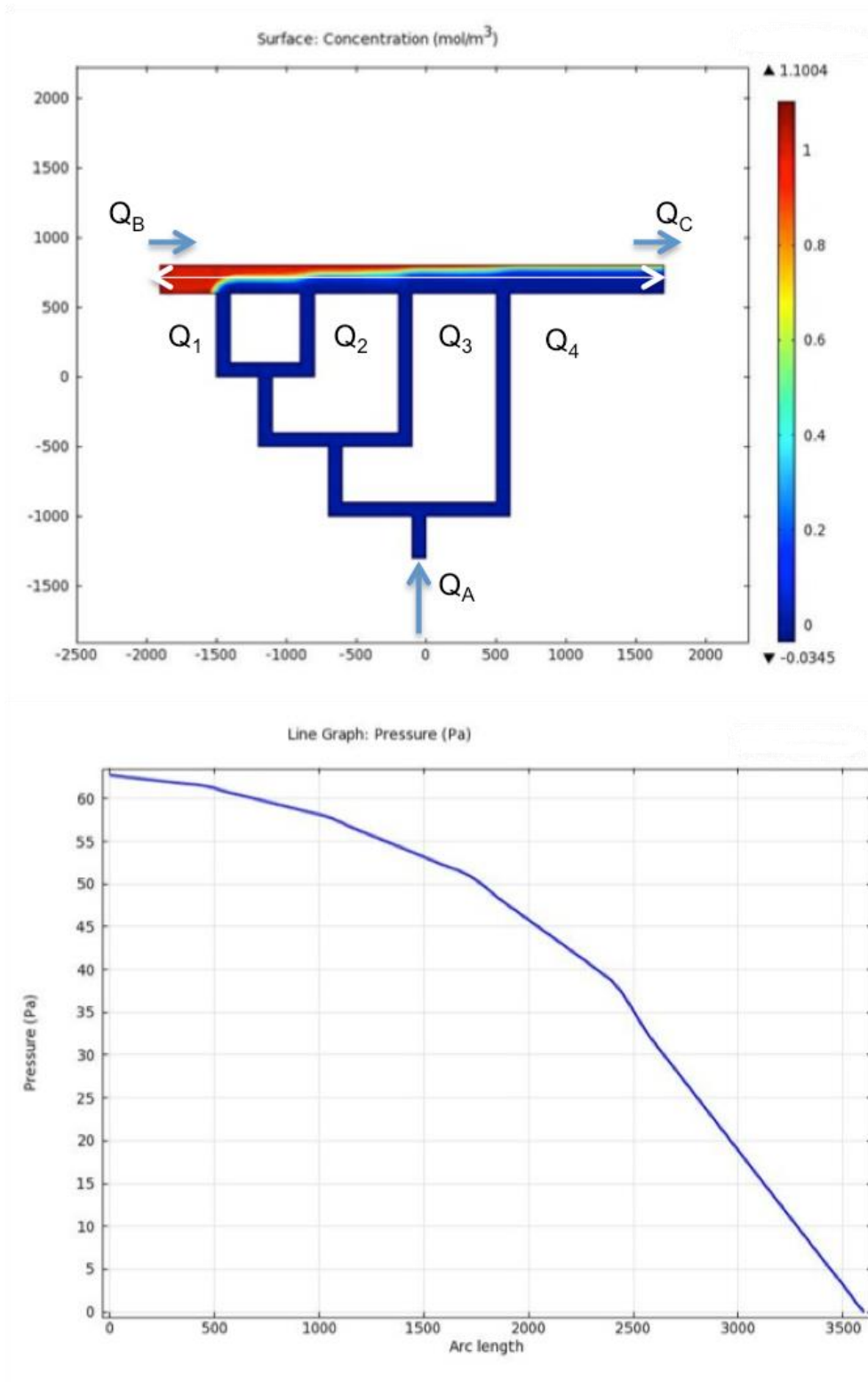


Figure 22: FEM model of SFM with four branches: use of SFM to reduce the effect of hydraulic blockage due the pressure generated at mixing node. Surface concentration of two liquids is shown (top). In particular, bioreagent (red) is compressed toward the top wall of the horizontal channel when in contact with the sample water (blue) due the pressure generated at mixing nodes. In this specific arrangement, pressure peak (bottom) is equivalent to 63 Pa: 42.73% less than the peak pressure built at the mixing node in Figure 19. Volumetric fluid

flow Q_B (bioreagent) and Q_A (sample) were set respectively at $7\mu\text{l}/\text{min}$ and $70\mu\text{l}/\text{min}$ at the two inlets. Applying a stepped-flow mixer enabled a reduction in the differential pressure between the two fluids being mixed. This enabled effective mixing while minimizing the risk of hydraulic blockage.

According to the specific arrangements shown in Figure 20 and Figure 22, applying the SFM enables a reduction of the peak pressure at mixing node when compared with a single mixing node of a T-connection as shown in Figure 18. Pressure is thereby distributed through the mixing nodes.

Notably, variation of the cross sectional area A_i of the branches in proximity of mixing nodes ultimately affect the pressure at mixing nodes, as provided in the above description and in Equations 4 and 5. The arrangements in the figures effectively minimises the risk of hydraulic blockage.

In conclusion, although the above mathematical analysis and simulation do not take into account the internal surface roughness of the channels as well as the effect of the distance between mixing node, it demonstrates that the hydraulic blockage could be effectively minimized by dividing the volumetric fluid flow Q_A through the branches. The result is a mixing with a distributed pressure over the mixing points. Consequently, backpressure generated at the mixing nodes is reduced.

2.7 SEGMENTED FLOW TEST

Bacteria aggregate in robust communities known as biofilm which are universally present in natural environments (Hall-Stoodley *et al.* 2004). The biofilm, by contrast, is a complex architecture of microchannels (Cho *et al.* 2007) comprising an agglomeration of microorganisms; and extracellular polymeric substances, such as DNA, polysaccharides, and proteins (Lear & Lewis 2012). It is well acknowledged that bacteria undergo profound changes to mutate from planktonic cells (free swimming) to part of the complex structure of the biofilm (O'Toole *et al.* 2000). It is also acknowledged that bacteria are able to generate chemical signals to change the structure of the biofilm (Higgins *et al.* 2007). When in the presence of mature biofilms, active bacteria which are part of the biofilm are more resistant to biocidal treatments, for example they may develop a specific phenotype resistant to biocide treatments (Mah & O'Toole 2001).

Biofilms may contaminate devices, medical implants, food facilities, and microfluidic devices (Costerton and Stewart, 2001) posing a high risk of contamination inside microfluidic ducts (Hall-Stoodley *et al.* 2004). It is recommended to counteract rather than treat biofilm development: a variety of strategies, such as biocidal compounds (e.g., antibiotics, silver ions, salts, etc.) and adhesion inhibitor (e.g., low polarizable materials, zwitterionic, mixed-charge, low surface energy, and amphiphilic materials), may be used to counteract or treat biofilm formation (Zhao *et al.*, 2009; Jiang and Cao, 2010; Epstein *et al.* 2013).

The method of formation of biofilm may be summarised in two steps. Initially, colonies of bacteria adhere to a substrate using fundamental physico-chemical mechanisms, such as long-distance Van der Waals forces, electrostatic forces, and Lewis acid-base interactions (i.e. Lewis acids are electron-pair acceptors which interact with Lewis bases by sharing electrons to form adducts); and subsequently, bacteria develop cell adhesion for more resistant and

permanent bond (Abu-Lail & Camesano 2006; Bos *et al.* 1999). Therefore, to reduce initial adhesion of bacteria to substrates is necessary to minimise the effect of the fundamental physico-chemical mechanisms which cause the initial adhesion. This may be easily obtained by substituting the substrate with adhesion inhibitors, such as smooth materials with non-reactive surfaces (e.g., COC or PTFE) that minimize van der Waals interactions (Autumn *et al.* 2002). A novel technique such as slippery liquid-infused porous surface (SLIPS), which maintains extreme biofilm repellence, is currently not applicable for commercial microfluidic chips (Wong *et al.* 2011) and was not considered in this work. This technique may represent a future solution to avoid biofilm development in microfluidic chips.

It is worth to note that the viability of the bacteria may be affected when using materials, such as PTFE and COC, which have low oxygen permeability characteristics (Boedeker 2007; Shin *et al.* 2005). Oxygen is necessary to activate the process of quorum sensing and is critical to keep *Vibrio fischeri* alive (Stevens and Greenberg 1997). In such a case alternative methods to provide gas exchange are necessary: a two phases segmented flow may be used to provide oxygen exchange to the bioreagent. As an example, Martin *et al.* describes a technique for the cultivation of monoclonal cells in a Teflon microfluidic circuit by using segmented flow (Martin *et al.* 2003).

In our particular case of study, the viability of the bacteria over a PTFE microfluidic chip comprising a single long duct of 737mm in length, 350µm wide, and 300µm depth was assessed as explained in the following paragraphs. The design of the PTFE chip was the same as the one shown for the COC chip in **Figure 25**.

The PTFE Chip (**Figure 24**) was enclosed by clamping a 50 µm thick film of perfluoroalkoxy (Sigma Aldrich) with 7mm thick fused silica (PI-KEM) over the Teflon wafer with a bolted stainless-steel manifold housing.

The objective of this test was to produce a graph showing the light changes over a section of the milled PTFE under (i) laminar single-phase flow, (ii) segmented flow with air, and (iii) segmented flow with oil (sunflower oil).

The equipment was set up as shown in Figure 23. In particular, a microbial bioreactor with M18 microbial culture medium was autoclaved at a temperature of 121 °C for 20 min and allowed to cool before inoculation. Freeze dried *Vibrio fischeri* were inoculated into the microbial bioreactor when the microbial culture medium was at room temperature. The microbial culture was incubated at ambient temperature (~22°C), shaking at 80rpm for 72hrs. At this point, the microbial culture was visibly bright. The microfluidic chip was flushed with distilled water for 1 hour prior to perform the three tests.

The three tests are presented as follows:

- first test: the bioreagent fluid flow was set at 30 μ l/min, and pumped directly from the fermentor into the PTFE duct without mixing with blank and/or buffer solution. Variations of light intensity over a section of the milled PTFE duct were recorded using a NIKON SMZ 800 & IXon EMCCD Andor camera. Accordingly, a graph (Figure 26/B) was produced showing light changes over a section (in red) of the milled PTFE duct under laminar single-phase flow.
- second test: the bioreagent flow was set at 30 μ l/min and the gas fluid flow was monitored to be 30 μ l/min. Bioreagent was pumped directly from the fermentor into the PTFE duct without mixing with blank and/or buffer solution. Variations of light intensity over a section of the milled PTFE were recorded using a NIKON SMZ 800 & IXon EMCCD Andor camera. Accordingly, a graph (Figure 26/C) was produced showing light changes over a section of the milled PTFE duct under segmented flow with air.

- third test: the bioreagent flow was set at 30 μ l/min and the oil flow at 30 μ l/min. Bioreagent was pumped directly from the fermentor into the PTFE duct without mixing with blank and/or buffer solution. Variations of light intensity over a section of the milled PTFE duct were recorded using a NIKON SMZ 800 & Andor iXon3 897 Single Photon Detection EMCCD Camera. Accordingly, a graph (Figure 26/A) was produced showing light changes over a section of the milled PTFE duct under segmented flow with oil (sunflower oil).

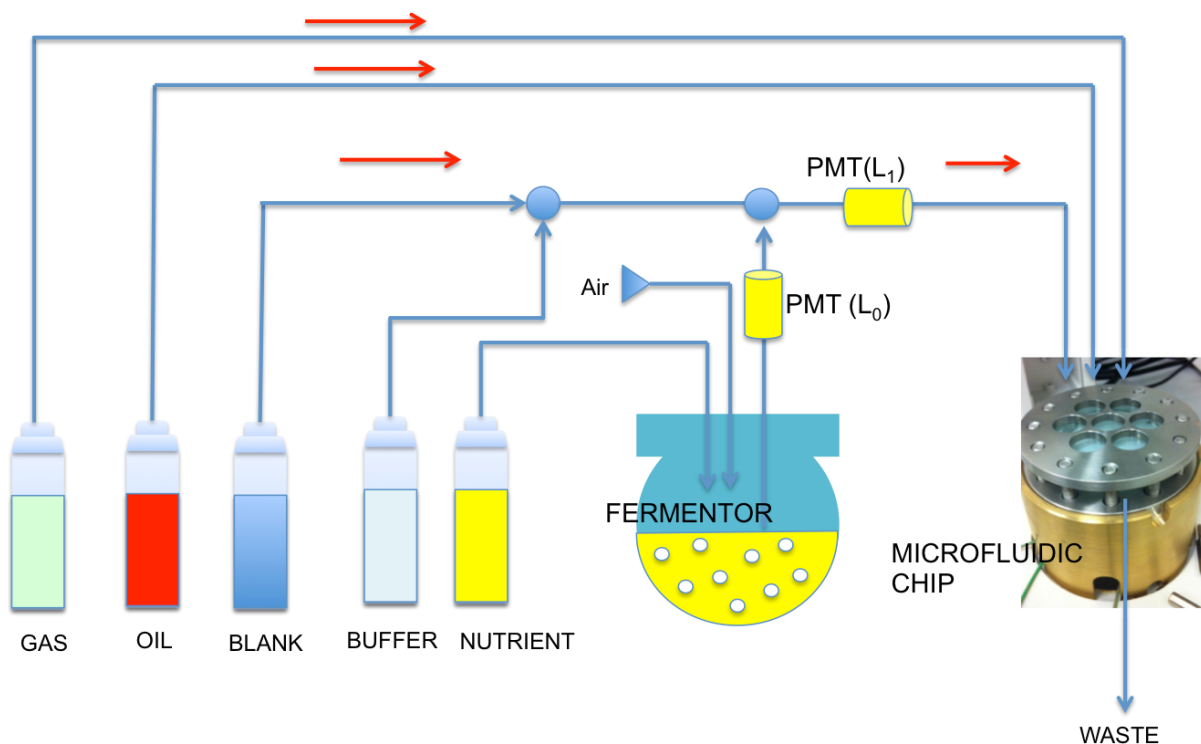


Figure 23: Equipment set up: the microbial bioreactor with continuous microbial culture of *Vibrio fischeri* in M18 microbial culture medium was constantly fed with a M18 microbial culture medium (NUTRIENT); it was aerated, stirred, and electronically controlled to maintain the expected growing condition. Light output was measured using photomultiplier tubes (PMTs). The reagent section comprised a vessel with distilled water (BLANK), a vessel containing air (GAS), a vessel containing brine (BUFFER), and a vessel containing sunflower oil (OIL). Every vessel was connected to a pumping system to generate a fluid flow into the PTFE microfluidic chip clamped in a metal case. Red arrows show the direction of the flow. The waste section (WASTE) comprised a waste tank. Variations of light intensity over a section of the milled PTFE were recorded using a NIKON SMZ 800 and an Andor iXon3 897 Single Photon Detection EMCCD Camera. The EMCCD

Camera was set to allow a single shot every 1 minute. Exposure time was set as follow: 1.5sec/0.06Hz, 10 accumulations, read rate 10 MHz at 14 bit, preamp gain 4.9x, and EM gain: 300%.

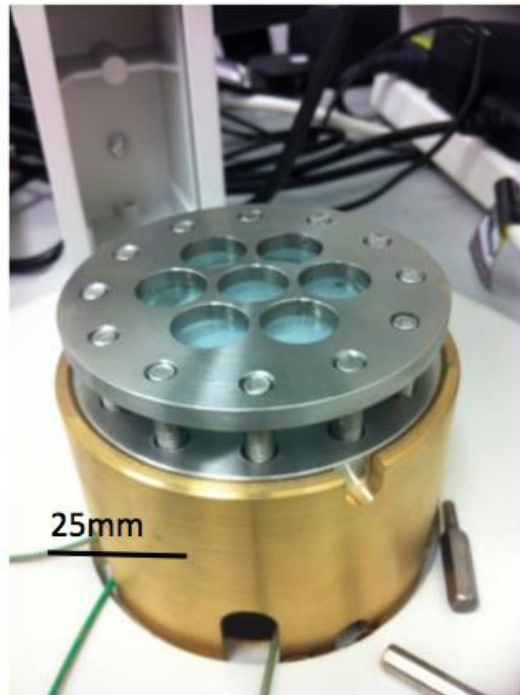


Figure 24: PTFE chip clamped in metal case: a PTFE chip was enclosed by clamping a 50 μ m thick film of perfluoroalkoxy (Sigma Aldrich) with 7mm thick fused silica (PI-KEM) over the Teflon wafer with a bolted, stainless-steel, manifold housing (Cardiff University). Internal ducts were produced using a micro-milling machine (LPKF Protomat C30). Size of the duct was estimated 737 μ m long, 350 μ m wide, and 300 μ m deep. Size of the planar Teflon PTFE wafer (Sigma Aldrich) was 50mm diameter, 4mm thick.

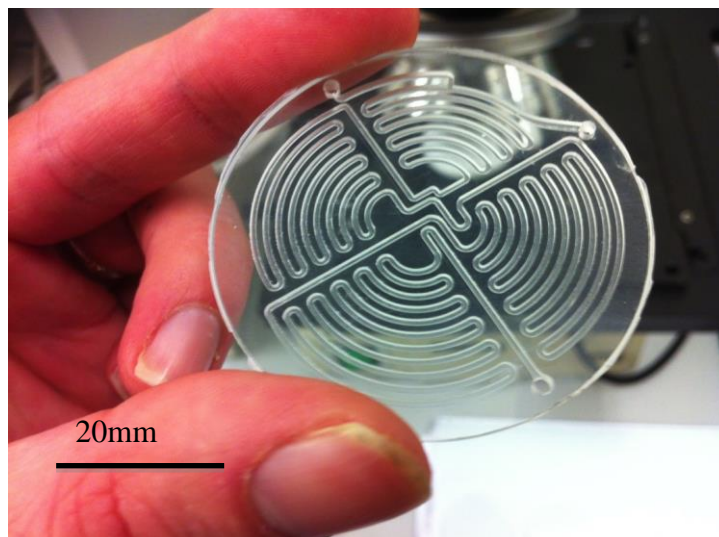


Figure 25: Example of milled chip design in COC. The design of the microfluidic duct in the picture is identical to the design of the PTFE chip in Figure 23, Figure 24 and Figure 26. In particular, the design comprises a

single long microfluidic duct having one inlet and one outlet. Size of the duct was estimated 737mm long, 350um wide, and 300um deep. Size of the planar COC wafer was 50mm diameter, 2mm thick.

2.7.1. RESULTS AND CONCLUSION

Three tests were performed in accordance with paragraph 2.7. In particular, it was observed the following as described henceforward.

During the laminar single-phase flow, an accumulation of bacteria along the duct walls was detected as shown in Figure 26/B and Figure 27. Peaks of light intensity were recorded in proximity of the sidewalls.

As it can be observed from Figure 27, light intensity is not zero in contiguous regions extending outside the duct walls. This effect is in consequence of the light diffraction per the presence of the 7mm thick fused silica (PI-KEM) over the Teflon wafer.

Ratio between H_1 (mean light intensity at the centre of the duct section) and H_2 (light intensity peak at the sidewall of the duct section) was equal to 0.45 across the section of the duct. A decay of mean bioluminescence along the whole microfluidic path was visibly observable (Figure 26/B).

On the other hand, during segmented flow with oil (sunflower oil), distribution of the light intensity across the section of the duct followed a Gaussian shape with substantially reduced accumulation of bacteria at the sidewalls. Indeed, peak of light intensity was observed in the middle of the duct (Figure 26/A and Figure 28).

Similarly to Figure 27, in Figure 28 light intensity is not zero in contiguous regions extending outside the duct walls. This effect is a consequence of the light diffraction effect per the presence of a 7mm thick fused silica (PI-KEM) over the Teflon wafer.

In yet another experiment, during segmented flow with air (see Figure 26/C and **Figure 29**) it was observed a reduced accumulation of bioreagent in proximity of duct walls when compared to laminar single-phase flow (Figure 26/B). Ratio H_1/H_2 was equal to 0.205, and

thus lower than the ratio estimated for laminar single-phase flow. The increase of bioluminescence along the whole microfluidic path was clearly observable as shown in Figure 26/C and **Figure 29**.

Again, as provided for Figure 27 and Figure 28, in **Figure 29** light intensity is not zero in contiguous regions extending outside the duct walls. This effect is a consequence of the light diffraction effect per the presence of a 7mm thick fused silica (PI-KEM) over the Teflon wafer.

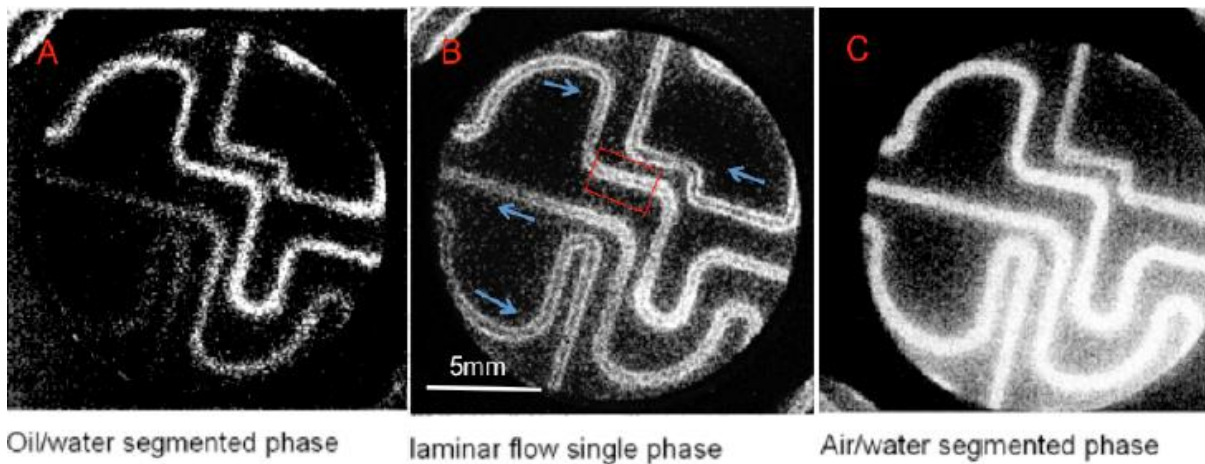


Figure 26: EMCCD camera view from central window of the clamped system in **Figure 24**. Representation in grey scale of single-phase laminar flow and segmented phase flow on a PTFE micromilled chip having identical design to the design in **Figure 25**. In particular, single frame shot (1/25s) of bioluminescent bacteria in segmented phase with sunflower oil (A), segmented flow with air (C), and single-phase laminar bioreagent flow (B). Note overall increased light emission in C. Direction of the fluid flow in the microchannels is represented with blue arrows in B (fluid flow start from top right arrow in picture). Section marked with red box in B has been processed to analyse the distribution of the bioluminescence across the channel, as shown in Figure 27, Figure 28 and Figure 29. Same section is applied also for A and C. Decay of the bioluminescence along the whole microfluidic path was visibly observable in B and A.

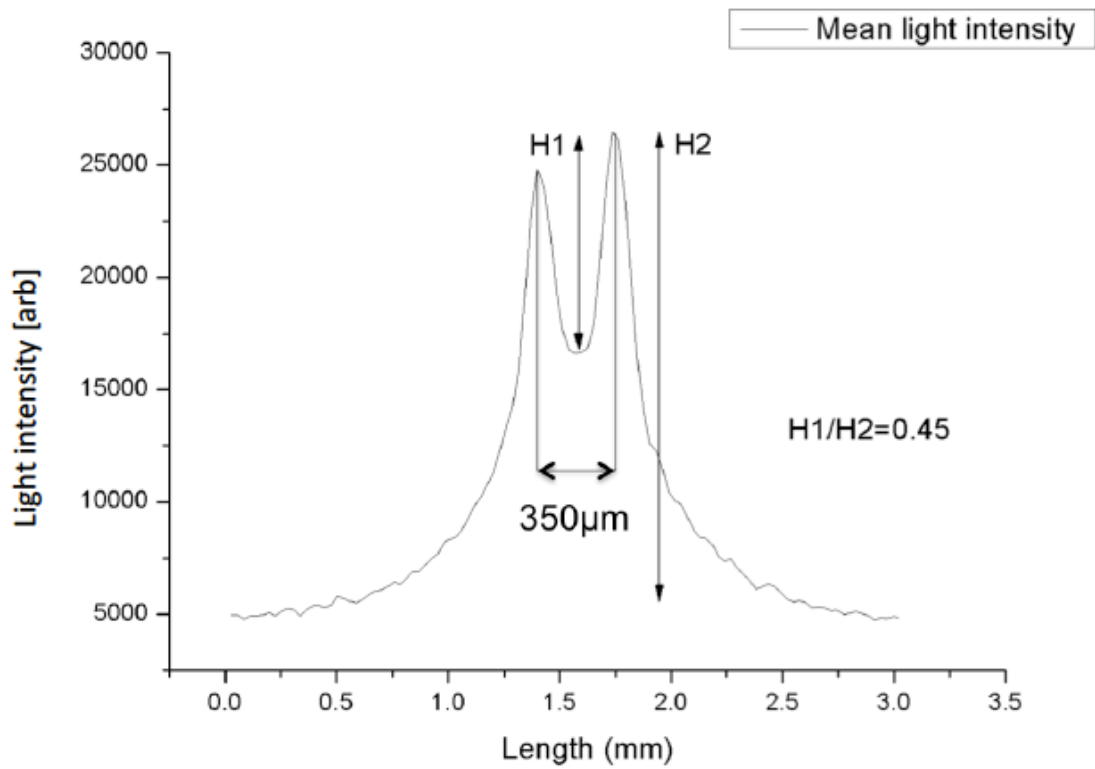


Figure 27: Mean bioluminescence of bacteria across the duct section during laminar single-phase flow of bioreagent: two peaks of bioluminescence are shown in proximity of the sidewalls as result of an accumulation of bacteria along the walls. Ratio between H1 (mean light intensity at the centre of the duct section) and H2 (highest light intensity peak at the wall of the duct section) is equal to 0.45. Axis X and Y represent respectively the length [mm] across the channel and the light intensity in arbitrary units. Duct size is 350µm.

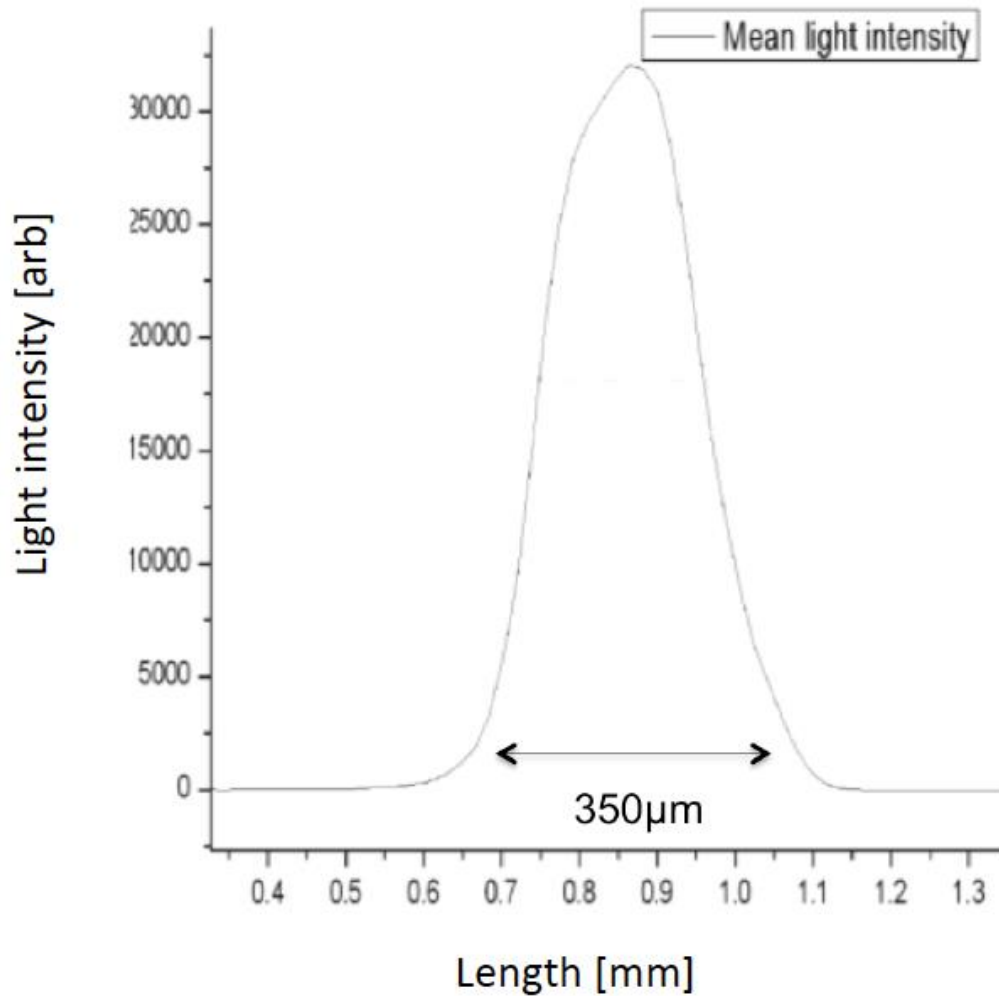


Figure 28: Mean bioluminescence of bacteria across the duct section during segmented flow with sunflower oil: a Gaussian distribution of the light intensity across the channel is shown in the picture. It may be evinced that the bacteria did not aggregate, or that minimal aggregation is present in proximity of the sidewalls; additionally, the peak of bioluminescence is observed in the middle of the duct. However, the drop of bioluminescence was visibly observable along the channel, most probably due oxygen starvation. Axis X and Y represent respectively the length [mm] across the channel and the light intensity in arbitrary units. Duct size is 350 μ m.

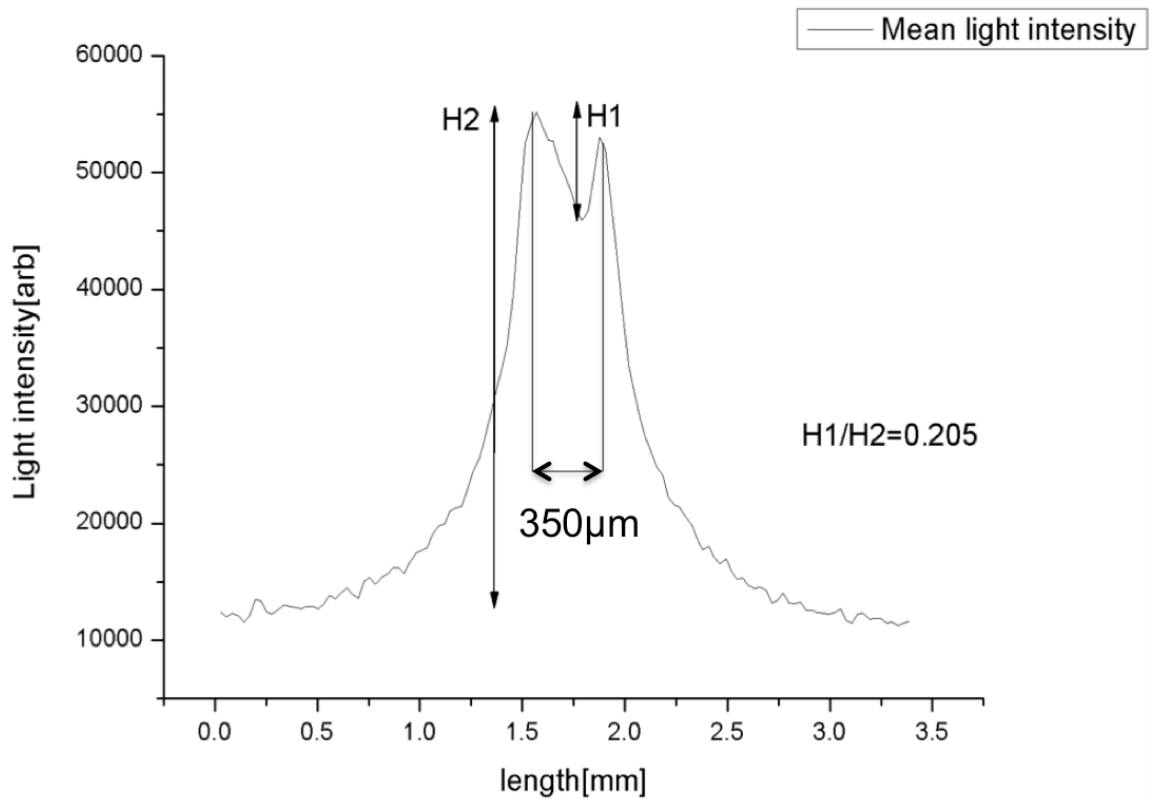


Figure 29: Mean bioluminescence of bacteria across the duct section during air/bioreagent segmented flow: two peaks of bioluminescence are shown in proximity of the sidewalls as consequence of an accumulation of bacteria along the walls. Ratio between H1 (mean light intensity at the centre of the duct section) and H2 (Highest light intensity peak at the wall of the duct section) is equal to 0.205. Axis X and Y represent respectively the length [mm] across the channel and the light intensity in arbitrary units. Duct size is 350µm.

As conclusion with the above results it was demonstrated that the presence of oxygen and the segmented flow are helpful mechanisms to maintain the microbial culture in a healthy condition and to reduce biofilm formation.

Specifically, with reference to the obtained results for the segmented fluid flow with oil, it was observed a substantially reduced accumulation of bioreagent in proximity of duct walls. Although this is less evident in the results obtained for segmented flow with air (note the ratio H_1/H_2 in **Figure 29** is less than H_1/H_2 in **Figure 27**), it appears that in both cases there are

more bacteria present in the middle region of the duct than when in laminar single-phase flow.

Further, with reference to the segmented flow with oil, drop of the light intensity along the whole microfluidic channel (Figure 26/A) was observed. In addition to this, it is well known that diffusivity of the oxygen in sunflower oil has a low value (180 mg/kg at 1 Bar, and 25°C) (Gunstone & Padley 1997).

Therefore it could be concluded that the insufficiency of oxygen inside the droplet and the minimal exchange of oxygen in the oil/bioreagent phase were most probably the main causes of the drop of the light intensity along the whole microfluidic channel (Figure 26/A). Indeed, it was conceptualised that bacteria had gradually lost their bioluminescence due oxygen starvation as consequence of the depletion of oxygen inside the confined space of a droplet.

As overall conclusion to this section, oil/bioreagent segmented fluid flow is a promising transport system that may substantially reduce biofilm formation and provide an improved exchange of oxygen in the oil/bioreagent if an appropriate oil having higher diffusivity coefficient than sunflower oil is used. This can be achieved i.e. with fluorocarbon-based fluid, as e.g. Fluorinert sold by 3M.

However, per the result of the present experiments carried in this section and per economic reasons related to the use of fluorocarbon-based fluid it was concluded that air/bioreagent segmented fluid flow may be the better option for the miniturised analyser.

Accordingly, air/bioreagent segmented fluid flow has the following potential:

- to enhance reaction due the internal mixing;
- to carry oxygen necessary to maintain a healthy environment for bacteria; and

- to avoid biofilm formation by reducing the amount of bacteria in contact with the duct side walls.

CHAPTER 3. GENERAL DISCUSSION

3.1 SIGNIFICANCE, LIMITATION AND FUTURE WORK

The high cost and large dimension of the commercially available CTM have stimulated a research towards a cheaper and portable version of this sensing device.

Although common research for portable devices has been particularly pushed toward the development of miniturised electronic tongues (Marco *et al.* 2006; Eicher & Merten 2011; Tian & Finehout 2009), in this work we focused on a miniaturised version of the CTM, NANOTOX, which comprises microfluidic systems and shares the same detection principle of the commercially available CTM.

Based on a predetermined set of initial requirements necessary to reduce the size of the system, and accordingly to the objectives of the research, an investigation that resulted in discrete number of improvements to the CTM has been presented in this disclosure. This list of technical improvements, as an outcome of two years' worth of research on the development of a new water toxicity analyser "NANOTOX" are briefly summarised as provided hereinafter.

Accordingly to a first improvement, a viable thermoplastic was selected among a set of potential candidates. In particular, Cyclic Olefin Copolymer (COC) demonstrated to be the closest match to the initial requirements for its characteristics, such as excellent transparency, low water absorption, biocompatibility, resistance to acids and alkalis, hydrophobicity, amenability to surface treatments, and amenability to sterilization procedures.

Accordingly to a second improvement, it was proposed an alternative system to preserve bacteria in substitution to the continuous microbial culture bioreactor used in the CTM. As provided in this work, the introduction of chilled bioreagent has the advantage of removing the presence of the bioreactor; thereby, reducing the need of complicated pump control

systems, necessary to accurately control the volume of the bioreactor, and eliminating the need of maintaining a continuous microbial culture under ideal conditions.

Accordingly to a third improvement, an assessment of existing pumping technologies was performed to find an adequate pumping system in accordance with the initial requirements. In particular, it was demonstrated through an experiment that the use of a vibrating membrane gas pump together with a glass container, and a fluid flow restrictor followed by a microdispensing controlling valve was sufficient to produce a constant fluid flow of few $\mu\text{l}/\text{min}$ over extended periods of time (weeks).

Accordingly to a fourth improvement, an investigation on a possible method to reduce the hydraulic blockage was performed. Hydraulic blockage occurs as a consequence of the backpressure generated when two volumetrically different fluid flows ($Q_a \gg Q_b$) converge at a mixing point. It was theoretically demonstrated that by applying a stepped flow mixer would minimize the risk of hydraulic blockage.

Accordingly to yet a fifth improvement, it was demonstrated that segmented fluid flow with air could be an helpful mechanisms, when applied to the microfluidic path of NANOTOX, to maintain the microbial culture in a healthy condition and to reduce biofilm formation.

However, despite the number of improvement described herein, further studies are now required in order to optimise and develop a full prototype most suited to on site practice.

For example, further improvement may be required to study alternative viable materials that may be used in the future such as PTFE, FEP, PFA if further developed so to be more amenable to bonding and mass production. These thermoplastic materials benefit of a strong hydrophobicity, acting as adhesion inhibitor materials, that when in combination with segmented flow with air may maintain bioreagent aerated and further reduce biofilm

formation. Indeed, the necessity to prevent, rather than treat, biofilm development and alternative methods to provide gas exchange are fundamental to maintain healthy bacteria during the detection stages.

As another example, further improvement may be done with respect to the transporting mechanism in the microfluidic duct. For example, oil/bioreagent segmented fluid flow may be further improved with the use of an appropriate oil with higher oxygen diffusivity coefficient, e.g. fluorocarbon-based fluid, and an appropriate mechanism to recycle fluorocarbon based fluid.

Alternatively, performed experiments in reference to the transporting mechanism in the microfluidic duct, may be further improved by providing different analysis for segmented fluid flow with air in function of controlled surface roughness of the internal duct.

As yet another example, further improvement may be done in respect to the use of electronic feedback or feedforward system to improve control over the dispensed fluid flow, and by using less expensive photodetectors in substitution to PTMs.

Finally, NANOTOX essentially inherits the same major drawback of biomonitors based on living organism, such as the CTM. Indeed, as specified in this work, there is no clear link between the harm to living organisms and the hazard for humans (e.g., genotoxicants, endocrine disruptors, pathogens, etc.).

As an example, hazard for humans such as pathogens may not be detected by the CTM or NANOTOX. This represents a great limitation, as these hazards are not an insignificant public health issue. It is appraised that pathogens are directly responsible for 15 Million deaths every year. They may be easily transported into the water distribution network.

Therefore, prevention systems which allow rapid point of care diagnosis are currently in demand (Tian & Finehout 2009).

In addition to that, NANOTOX detects only severe toxicity and not chronic toxicity; pollutants provoking chronic effects may be recognized only with laboratory-based in vitro assays (Flückiger-Isler *et al.* 2004; Sonneveld *et al.* 2005; Eltzov *et al.* 2009).

Further development may thus been done with respect to the above to provide NANOTOX with necessary equipment to detect genotoxicants, endocrine disruptors, pathogens, and eventually pollutant provoking chronic effect.

In conclusion to this work there is still a long way to go and room for further improvements for the realization of a cost effective continuous and broad water quality monitor as a tailored combination of microfluidic systems and in accordance with the initial requirements. Likewise, more should be done to provide a cost effective final system including all the technical development, and eventually future developments mentioned above.

Additionally, it is worth to mention that during this research, as consequence of the number of development and widespread focus toward multiple technical aspects, continuous change of direction have been done resulting in a delay to the final objective of providing an ultimate solution to the critical need for a small, fast, and more economical method to detect water toxicity.

There thus would appear, in hindsight, that more effort should have been provided to define a clear initial path to follow, and to nonetheless leave greater flexibility to the management of the present project. With this final considerations in mind there could have been a substantial decrease in the delay that would eventually have led to the provision of a final system within the two years timeframe.

ANNEXES

Table 11: Thermoplastics selection.

Name	Characteristics	Biocompatibility	Water θ ($^{\circ}$)	Solvent resistant
Poly (methyl methacrylate) (PMMA)	<ul style="list-style-type: none"> • Inexpensive, • Optical transparent, • Low water absorption, • Easy to manufacture. <p>(MIT 2004; Zeng <i>et al.</i> 2002)</p>	YES	63	Good
Cyclic Olefin Copolymer (COC)	<ul style="list-style-type: none"> • Low density, • Excellent transparency (92%), • Low water absorption, • Biocompatible, • Solvent resistant, • Good flowability, • Hydrophobicity, • Production by common hot embossing technique, • Amenability to surface treatments, • Widely used in the pharmaceutical industry, • Low glass transition temperature, • Surface energy may be changed by plasma treatment and remain modified for several days, 	YES	85	Excellent

	<ul style="list-style-type: none"> • Sterilizable by autoclaving or gamma radiating, • Heat resistant. <p>(Shin <i>et al.</i> 2005; Fink 2010)</p>			
Polyvinyl Chloride (PVC)	<ul style="list-style-type: none"> • Cheap and strong, • Problems on discarding, • Compatible with many solvents. <p>(Titow and Titow 1984; Wilkes <i>et al.</i> 2005)</p>	Yes	83	Good
Polydimethylsiloxane (PDMS)	<ul style="list-style-type: none"> • Incompatible with a wide range of solvents, especially organic, • Thermoset, • Good contact angle, • Large biomolecules tend to stick to its surface, • Small molecules may seep in and out of its bulk, • Viscoelastic, • Good chemical stability, • Used for imprinting. • Optically clear, • Inert, • Non-toxic, • Non-flammable, • Not a viable option for mass 	Yes	110	Bad

	<p>production.</p> <p>(Saia <i>et al.</i> 2011; Lötters <i>et al.</i> 1997)</p>			
<p>Polytetrafluoroethylene (PTFE)</p>	<ul style="list-style-type: none"> • Chemically inert, • Thermally resistant up to 260°C, • Hydrophobic and oleophobic, • High tensile strength, • Autoclavable, • Biocompatible. <p>(Ren <i>et al.</i> 2011; Blumm <i>et al.</i> 2010)</p>	Yes	111	Excellent
<p>Perfluoroalkoxy (PFA)</p>	<ul style="list-style-type: none"> • Similar to PTFE, • Melt-processable, • Flexible, • PFA is more affected by water absorption and weathering than FEP, • Low adsorption of biomolecules onto duct walls, • Low transparency. <p>(Row Inc. [no date]; Boedeker, 2007)</p>	Yes,	111	Excellent
<p>Fluorinated ethylene propylene (FEP)</p>	<ul style="list-style-type: none"> • FEP is softer than PTFE; • Highly transparent, • Resistant to sunlight, • Similar to PFA, 	YES	108	Excellent

	<ul style="list-style-type: none"> • Sealable with thermobonding technique, but both temperature and pressure need cautious controls, • Little adsorption of biomolecules, • Difficult to thermobond. <p>(Boedeker 2007)</p>			
Polyvinylidene Fluoride (PVDF)	<ul style="list-style-type: none"> • Low thermal conductivity, • Solvent resistance, • Mechanical strength and toughness, • Low permeability to most gases and liquids, • Used as porous Hydrophobic membrane, • Semi crystalline polymer, • Heat resistance, • Pyroelectric, piezoelectric and ferroelectric properties, • It undergoes crystallization during melting/cooling, • Can be gamma radiated. <p>(Kawai 1969; Porex Inc. [no date])</p>	Yes	89	Excellent
Poly (oxymethylene)	<ul style="list-style-type: none"> • High stiffness, • Low friction, • Excellent dimensional 	Yes	76.8	Good

Glycol (POM)	<p>stability,</p> <ul style="list-style-type: none"> • Very difficult to bond. <p>(Snogren 1974)</p>			
polyamide-imide (PAI)	<ul style="list-style-type: none"> • High temperature resistance, • Low chemical resistance, • Good for membrane based gas separations and thin films. <p>(Torlon [no date]; Encyclopedia Britannica [no date]; Goodfellow Inc. [no date])</p>	Yes	76	Poor
Polybutylene Terephthalate (PBT)	<ul style="list-style-type: none"> • Semi crystalline resin, • Tough, • PBT is often preferred over Polyethylene Terephthalate (PET) because it crystallizes faster, • PBT is sensitive to hot water, strong bases, oxidizing acids, and ketones, • PBT is notch sensitive. <p>(Steinwall [no date]; Stein and Misra 1980; van Bennekom and Gaymans 1997)</p>	/	/	Poor
polyethylene terephthalate	<ul style="list-style-type: none"> • Good optical proprieties, • Low rigidity, • Low surface energy, 	Yes	72	Excellent

(PET)	<ul style="list-style-type: none"> • Disposable plastic, • Can be gamma radiated. <p>(Hoff and Mathers, 2010)</p>			
Polycarbonates (PC)	<ul style="list-style-type: none"> • Optical transparency, • Easily worked, moulded, and thermoformed, • Stronger than PMMA, • Good temperature range, • High impact resistance, • Poor resistance to certain organic solvents, • UV absorbance, • Can be autoclaved, • Gamma radiation cause aging and discolouring. <p>(Howdeshell <i>et al.</i> 2003; Parvin and Williams 1975)</p>	Yes	71	Good
Polyethylene (PE)	<ul style="list-style-type: none"> • Solvent resistant, • Porous (holes diameter ranging from 7µm to 150µm), • Stable under gamma radiation, • Disposable plastic, • Translucent, <p>(Hoff and Mathers 2010)</p>	Yes	96	Fair

<p>Polyether ether ketone (PEEK)</p>	<ul style="list-style-type: none"> • Heat resistant, • Water resistant, • Solvent resistant, • Excellent electrical insulating properties, • High fatigue strength, • Radioactive resistance, • High oxygen index, • Non transparent. <p>(PRNewswire 2010; Lauzon 2012)</p>	<p>Yes</p>	<p>71</p>	<p>Excellent</p>
<p>Polyethersulfone (PES)</p>	<ul style="list-style-type: none"> • Melt-processable at very high temperature (300 °C), • Transparent, • Porous. <p>(Hickner <i>et al.</i> 2004)</p>	<p>/</p>	<p>/</p>	<p>Good</p>
<p>Polypropylene (PP)</p>	<ul style="list-style-type: none"> • Good optical proprieties, • Solvent resistant, • Heat resistant (can be autoclaved), • PP stiffer and more resistant to creep compared to polyethylene (PE). <p>(Bayasi & Zeng 1993; Maier & Calafut 1998; Porex Inc. 2011a)</p>	<p>/</p>	<p>102</p>	<p>Good</p>

Polysulfone (PSU)	<ul style="list-style-type: none"> • Excellent optical proprieties, • Strong bonding by heating, • Can be gamma radiated. <p>(Wu <i>et al.</i> 2004; Chen <i>et al.</i> 2008)</p>	Yes	87	Poor
----------------------	--	-----	----	------

REFERENCES AND BIBLIOGRAPHY

Abu-Lail, N.I. & Camesano, T.A., 2006. 'Specific and nonspecific interaction forces between Escherichia coli and silicon nitride, determined by poisson statistical analysis'. *The ACS Journal of Surfaces and Colloids*, 22(17), pp.7296–301. Available at: <http://www.ncbi.nlm.nih.gov/pubmed/16893229> [Accessed November 28, 2013].

Ashbolt, N.J., 2004. 'Microbial contamination of drinking water and disease outcomes in developing regions'. *Toxicology*, 198(1), pp.229–238. Available at: <http://www.sciencedirect.com/science/article/pii/S0300483X04000952> [Accessed November 1, 2013].

Autumn, K. *et al.*, 2002. 'Evidence for van der Waals adhesion in gecko setae'. *Proceedings of the National Academy of Sciences of the United States of America (PNAS)*, 99(19), pp.12252–6. Available at: <http://www.pnas.org/content/99/19/12252.abstract> [Accessed November 19, 2013].

Babbitt, H.E. & Doland, J.J., 1955. *Water Supply Engineering* McGraw-Hill, ed., Available at: http://books.google.it/books/about/Water_Supply_Engineering.html?id=X-UmAAAAMAAJ&redir_esc=y.

Bayasi, Z. & Zeng, J., 1993. 'Properties of polypropylene fiber reinforced concrete'. *ACI Materials Journal*, 90(6), pp.605 – 610. Available at: <http://www.concrete.org/Publications/ACIMaterialsJournal/ACIJJournalSearch.aspx?m=details&ID=4439> [Accessed April 28, 2013].

Van Bennekom, A.C.M. & Gaymans, R.J., 1997. 'Amide modified polybutylene terephthalate: structure and properties'. *Polymer*, 38(3), pp.657–665. Available at: <http://www.sciencedirect.com/science/article/pii/S0032386196005538> [Accessed December 6, 2013].

Blumm, J. *et al.*, 2010. 'Characterization of PTFE Using Advanced Thermal Analysis Techniques'. *International Journal of Thermophysics*, 31(10), pp.1919–1927. Available at: <http://dx.doi.org/10.1007/s10765-008-0512-z> [Accessed April 29, 2013].

- Boedeker Plastics Inc., 2014. 'PTFE, FEP, and PFA Specifications'. Available at: http://www.boedeker.com/feppfa_p.htm [Accessed April 29, 2014].
- Bogges, B., 2001. 'Mass Spectrometry Desk Reference (Sparkman, O. D.)'. *Journal of Chemical Education*, 78(2), p.168. Available at: <http://dx.doi.org/10.1021/ed078p168.2> [Accessed November 3, 2013].
- Borcherding, J. & Wolf, J., 2001. 'The influence of suspended particles on the acute toxicity of 2-chloro-4-nitro-aniline, cadmium, and pentachlorophenol on the valve movement response of the zebra mussel (*Dreissena polymorpha*)'. *Archives of Environmental Contamination and Toxicology*, 40(4), pp.497–504. Available at: <http://www.ncbi.nlm.nih.gov/pubmed/11525492> [Accessed November 30, 2013].
- Bos, R. *et al.*, 1999. 'Physico-chemistry of initial microbial adhesive interactions, its mechanisms and methods for study'. *FEMS Microbiology Reviews*, 23(2), pp.179–230. Available at: <http://doi.wiley.com/10.1111/j.1574-6976.1999.tb00396.x> [Accessed June 4, 2014].
- Bremere, I. *et al.*, 2001. 'How water scarcity will effect the growth in the desalination market in the coming 25 years'. *Desalination*, 138(1), pp.7–15. Available at: <http://www.sciencedirect.com/science/article/pii/S0011916401002399> [Accessed November 1, 2013].
- Brown, L.R., 2005. *Outgrowing the earth: the food security challenge in an age of falling water tables and rising temperatures*, Earthscan. Available at: http://books.google.it/books/about/Outgrowing_the_Earth.html?id=9rGgN8fwuPEC&redir_esc=y [Accessed October 31, 2013].
- Bulich, A.A. *et al.*, 1990. 'The luminescent bacteria toxicity test: Its potential as an in vitro alternative'. *Journal of Bioluminescence and Chemiluminescence*, 5(2), pp.71–77. Available at: <http://onlinelibrary.wiley.com/doi/10.1002/bio.1170050202/abstract> [Accessed October 31, 2013].
- Chen, C.S. *et al.*, 2008. 'Shrinky-Dink microfluidics: 3D polystyrene chips'. *Lab on a Chip*, 8(4), pp.622–4. Available at: <http://www.ncbi.nlm.nih.gov/pubmed/18369519>.

Costerton, J.W. & Stewart, P.S., 2001. 'Battling biofilms.' *Scientific American*, 285(1), pp.74–81. Available at: <http://www.ncbi.nlm.nih.gov/pubmed/11432197> [Accessed November 28, 2013].

Crozier, W.W., 1985. 'Observations on the food and feeding of the angler-fish, *Lophim piscatorius* L., in the northern Irish Sea'. *Journal of Fish Biology*, 27(5), pp.655–665. Available at: <http://doi.wiley.com/10.1111/j.1095-8649.1985.tb03210.x> [Accessed November 30, 2013].

Dasgupta, S. *et al.*, 2002. 'Confronting the Environmental Kuznets Curve'. *The Journal of Economic Perspectives*, 16(1), pp.147–168. Available at: <http://www.jstor.org/discover/10.2307/2696580?uid=2&uid=4&sid=21102853229581>.

EEC, 1981. *EU directives relating to water quality*, Europe: http://europa.eu/index_en.htm. Available at: <http://www.doeni.gov.uk/niea/water/water-policy/directives.htm> [Accessed November 2, 2013].

Eicher, D. & Merten, C.A., 2011. 'Microfluidic devices for diagnostic applications'. *Expert review of Molecular Diagnostics*, 11(5), pp.505–19. Available at: <http://www.ncbi.nlm.nih.gov/pubmed/21707459> [Accessed June 5, 2014].

Eltzov, E. *et al.*, 2009. 'Flow-through real-time bacterial biosensor for toxic compounds in water'. *Sensors and Actuators B: Chemical*, 142(1), pp.11–18. Available at: <http://www.sciencedirect.com/science/article/pii/S0925400509006546> [Accessed January 28, 2014].

Epstein, A.K. *et al.*, 2013. 'Biofilm attachment reduction on bioinspired, dynamic, micro-wrinkling surfaces'. *New Journal of Physics*, 15(9), p.095018. Available at: <http://iopscience.iop.org/1367-2630/15/9/095018/article/> [Accessed November 28, 2013].

Farideh, A. *et al.*, 2012. 'A Comprehensive Study of Micropumps Technologies'. *International Journal of Electrochemical Science*, 7, pp.9765 – 9780. Available at: <http://www.electrochemsci.org/papers/vol7/71009765.pdf>.

Flückiger-Isler, S. *et al.*, 2004. 'Assessment of the performance of the Ames II assay: a collaborative study with 19 coded compounds'. *Mutation research*, 558(2), pp.181–97.

Available at: <http://www.ncbi.nlm.nih.gov/pubmed/15036131> [Accessed November 30, 2013].

Global Industry Analysts, 2012. 'Global Drinking and Wastewater Treatment Chemicals Industry - market research report', p.793. Available at: <http://www.reportlinker.com/p0397822-summary/Global-Drinking-and-Wastewater-Treatment-Chemicals-Industry.html> [Accessed May 13, 2013].

Goel, P.K., 2006. *Water Pollution - Causes, Effects and Control*, New Delhi: New Age International. Available at: http://books.google.it/books/about/Water_Pollution.html?id=n1Gix9EjCzMC&redir_esc=y [Accessed October 31, 2013].

Goodfellow Inc., 2014. 'Polyamide/imide - online catalogue'. Available at: <http://www.goodfellow.com/E/Polyamide-imide.html> [Accessed April 29, 2013].

Government of Wales, 2010. *The Water Supply (Water Quality) Regulations 2010*, UK: legislation.gov.uk. Available at: http://www.legislation.gov.uk/wsi/2010/994/pdfs/wsi_20100994_en.pdf.

Gross, A.C. & Deneen, M.A., 2005. 'The Global Market for Water Treatment Products'. *Business Economics*, 40(1), pp.50–56. Available at: <http://www.palgrave-journals.com/doi/10.2145/20050108> [Accessed November 1, 2013].

Gunstone, F.D. & Padley, F.B., 1997. *Lipid Technologies and Applications*, CRC Press. Available at: <http://books.google.com/books?id=MccA-I5PgIsC&pgis=1> [Accessed January 2, 2014].

Hadeler, B. *et al.*, 1995. 'Gelrite and Agar Differently Influence Cytokinin-Sensitivity of a Moss'. *Journal of Plant Physiology*, 146(3), pp.369–371. Available at: <http://www.sciencedirect.com/science/article/pii/S0176161711820717> [Accessed November 6, 2013].

Hall-Stoodley, L. *et al.*, 2004. 'Bacterial biofilms: from the natural environment to infectious diseases'. *Nature reviews. Microbiology*, 2(2), pp.95–108. Available at: <http://www.nature.com/nrmicro/journal/v2/n2/abs/nrmicro821.html> [Accessed February 28, 2013].

Hickner, M.A. *et al.*, 2004. 'Alternative Polymer Systems for Proton Exchange Membranes (PEMs)'. *Chemical Reviews*, 104(10), pp.4587–4612. Available at: <http://dx.doi.org/10.1021/cr020711a> [Accessed April 8, 2013].

Higgins, D.A. *et al.*, 2007. 'The major *Vibrio cholerae* autoinducer and its role in virulence factor production'. *Nature*, 450(7171), pp.883–6. Available at: <http://www.ncbi.nlm.nih.gov/pubmed/18004304> [Accessed November 14, 2013].

Hinman, F., 1971. 'Obstruction: back pressure or residual volume and laminar flow'. *The Journal of Urology*, 105(5), pp.702–8. Available at: <http://www.ncbi.nlm.nih.gov/pubmed/5577216> [Accessed December 6, 2013].

Hoekstra, A.Y. & Chapagain, A.K., 2006. 'Water footprints of nations: Water use by people as a function of their consumption pattern'. *Water Resources Management*, 21(1), pp.35–48. Available at: <http://link.springer.com/10.1007/s11269-006-9039-x> [Accessed November 1, 2013].

Hoff, R. & Mathers, R.T., 2010. *Handbook of Transition Metal Polymerization Catalysts* available at, Hoboken, NJ, USA: John Wiley & Sons, Inc. Available at: <http://onlinelibrary.wiley.com/book/10.1002/9780470504437> [Accessed April 28, 2013].

HoJung, C. *et al.*, 2007. 'Self-organization in high-density bacterial colonies: efficient crowd control' J. McGrath, ed. *PLoS Biology*, 5(11), p.302. Available at: <http://dx.plos.org/10.1371/journal.pbio.0050302> [Accessed November 15, 2013].

De Hoogh, C.J., 2006. 'HPLC-DAD and Q-TOF MS techniques identify cause of *Daphnia* biomonitor alarms in the River Meuse'. *Environmental science & technology*, 40(8), pp.2678–85. Available at: <http://www.ncbi.nlm.nih.gov/pubmed/16683608> [Accessed November 30, 2013].

Howdeshell, K.L. *et al.*, 2003. 'Bisphenol A is released from used polycarbonate animal cages into water at room temperature'. *Environmental Health Perspectives*, 111(9), pp.1180–1187. Available at: <http://www.ncbi.nlm.nih.gov/pmc/articles/PMC1241572/> [Accessed April 4, 2013].

Ian J, A. *et al.*, 2006. 'A “toolbox” for biological and chemical monitoring requirements for the European Union’s Water Framework Directive'. *Talanta*, 69(2), pp.302–322. Available

at: <http://www.sciencedirect.com/science/article/pii/S0039914005006636> [Accessed November 30, 2013].

Idel'chik, I.E. & Fried, E., 1996. *Handbook of Hydraulic Resistance* 3rd ed. Begell House, ed., Hemisphere Publishing, New York, NY. Available at: http://books.google.it/books/about/Handbook_of_Hydraulic_Resistance.html?id=Fvh6i4TipsgC&redir_esc=y [Accessed December 6, 2013].

Inglehart, R., 1995. 'Public support for environmental protection: Objective problems and subjective values in 43 societies'. *PS: Political Science and Politics*, 28(1), pp.57–72. Available at: <http://www.jstor.org/discover/10.2307/420583?uid=3737536&uid=2&uid=4&sid=21102820590657>.

Jereb, P. & Roper, C.F.E., 2005. *Cephalopods of the World: Chambered nautilus and sepioids (Nautilidae, Sepiidae, Sepiolidae, Sepiadariidae, Idiosepiidae, and Spirulidae)*, Food & Agriculture Org. Available at: <http://books.google.com/books?id=QkkjaSA1jKgC&pgis=1> [Accessed November 30, 2013].

Jiang, S. & Cao, Z., 2010. 'Ultralow-fouling, functionalizable, and hydrolyzable zwitterionic materials and their derivatives for biological applications'. *Advanced materials (Deerfield Beach, Fla.)*, 22(9), pp.920–32. Available at: <http://www.ncbi.nlm.nih.gov/pubmed/20217815> [Accessed November 6, 2013].

Johnson, D.L. *et al.*, 1997. 'Meanings of Environmental Terms'. *Journal of Environment Quality*, 26(3), p.581. Available at: <https://www.agronomy.org/publications/jeq/abstracts/26/3/JEQ0260030581> [Accessed February 28, 2013].

Ju, H. *et al.*, 2011. 'Assembly of Nanostructures for Taste Sensing'. *NanoBiosensing Biological and Medical Physics, Biomedical Engineering*, pp.349–364. Available at: http://link.springer.com/chapter/10.1007/978-1-4419-9622-0_12.

Karant, P.N. *et al.*, 2010. 'Modeling of single and multilayer polyvinylidene fluoride film for micro pump actuation'. *Microsystem Technologies*, 16(4), pp.641–646. Available at: <http://link.springer.com/article/10.1007/s00542-009-0996-x#page-1>.

Kawai, H., 1969. 'The Piezoelectricity of Poly (vinylidene Fluoride)'. *Japanese Journal of Applied Physics*, 8(7), pp.975–976. Available at: http://en.wikipedia.org/wiki/Polyvinylidene_fluoride [Accessed April 29, 2013].

Kessler, H.J. & Redmann, U., 1974. 'Experience with low temperature storage of bacteria and fungi'. *Infection*, 2(1), pp.29–36. Available at: <http://link.springer.com/10.1007/BF01642221> [Accessed June 4, 2014].

Kirby, B.J., 2009. *Micro and Nanoscale Fluid Mechanics: Transport in Microfluidic Devices* available at, Cambridge University Press. Available at: <http://www.cambridge.org/it/academic/subjects/engineering/thermal-fluids-engineering/micro-and-nanoscale-fluid-mechanics-transport-microfluidic-devices?format=HB> [Accessed May 14, 2013].

Kirby, B.J. *et al.*, 2002. 'Voltage-addressable on/off microvalves for high-pressure microchip separations'. *Journal of Chromatography A*, 979(1-2), pp.147–154. Available at: http://www.researchgate.net/publication/10977416_Voltage-addressable_onoff_microvalves_for_high-pressure_microchip_separations?ev=pub_cit [Accessed December 29, 2013].

Laser, D.J. & Santiago, J.G., 2004. 'A review of micropumps'. *Journal of Micromechanics and Microengineering*, 14(6), pp.R35–R64. Available at: <http://stacks.iop.org/0960-1317/14/i=6/a=R01> [Accessed December 18, 2013].

Lauzon, M., 2012. 'Diversified Plastics Inc., PEEK playing role in space probe'. *PlasticsNews.com*. Available at: <http://www.plasticsnews.com/headlines2.html?id=25366> [Accessed April 28, 2013].

Lear, G. & Lewis, G., 2012. *Microbial Biofilms: Current Research and Applications* 1st ed., Caister Academic Press. Available at: <http://www.amazon.com/Microbial-Biofilms-Current-Research-Applications/dp/1904455964>.

Li, X.-J.J. & Zhou, Y., 2013. *Microfluidic devices for biomedical applications*, Elsevier. Available at: <https://www.elsevier.com/books/microfluidic-devices-for-biomedical-applications/li/978-0-85709-697-5> [Accessed June 9, 2014].

Lindsay, S. & Kealey, D., 1987. *High performance liquid chromatography*, John Wiley and Sons, New York, NY. Available at: <http://www.osti.gov/scitech/biblio/7013902> [Accessed November 3, 2013].

Liu, K. *et al.*, 2010. 'Microfluidic Systems for Biosensing'. *Sensors*, 10, pp.6623–6661.

Livermore, C. & Voldman, J., 2004. 'Design and Fabrication of Microelectromechanical Devices'. *MIT*. Available at: <http://www.mit.edu/~6.777/matprops/pmma.htm> [Accessed April 29, 2013].

Lötters, J.C. *et al.*, 1997. 'The mechanical properties of the rubber elastic polymer polydimethylsiloxane for sensor applications'. *Journal of Micromechanics and Microengineering*, 7(3), pp.145–147. Available at: <http://iopscience.iop.org/0960-1317/7/3/017> [Accessed April 28, 2013].

Luoma, S.N. *et al.*, 2008. *Metal contamination in aquatic environments: science and lateral management*, Cambridge University Press. Available at: <http://www.cabdirect.org/abstracts/20083330272.html> [Accessed November 1, 2013].

Madigan, M. & Martinko, J., 2010. *Brock Biology of Microorganisms* 13th ed., Benjamin Cummings. Available at: <http://www.amazon.com/Brock-Biology-Microorganisms-13th-Edition/dp/032164963X> [Accessed April 29, 2013].

Mah, T.-F.C. & O'Toole, G.A., 2001. 'Mechanisms of biofilm resistance to antimicrobial agents'. *Trends in Microbiology*, 9(1), pp.34–39. Available at: [http://www.cell.com/trends/microbiology/fulltext/S0966-842X\(00\)01913-2](http://www.cell.com/trends/microbiology/fulltext/S0966-842X(00)01913-2) [Accessed November 28, 2013].

Maier, C. & Calafut, T., 1998. *Polypropylene: the definitive user's guide and databook*, William Andrew. Available at: <http://books.google.com/?id=AWaSJd9Non8C&pg=PA14> [Accessed April 28, 2013].

Marco, S. *et al.*, 2006. 'Multi-sensor array used as an “electronic tongue” for mineral water analysis'. *Sensors and Actuators B: Chemical*, 116(1), pp.130–134. Available at: <http://www.sciencedirect.com/science/article/pii/S0925400506001742> [Accessed November 6, 2013].

MarketLine, 2012. 'Water Utilities Global Industry Almanac MarketLine', p.595. Available at: <http://www.reportlinker.com/p0688971-summary/Water-Utilities-Global-Industry-Almanac-MarketLine.html> [Accessed May 13, 2013].

Martin, K. *et al.*, 2003. 'Generation of larger numbers of separated microbial populations by cultivation in segmented-flow microdevices'. *Lab on a chip*, 3(3), pp.202–7. Available at: <http://pubs.rsc.org/en/content/articlehtml/2003/lc/b301258c> [Accessed December 30, 2013].

Maxwell, S., 2012. '2012 Water Market review'. *Technoledge y strategy group*. Available at: <http://www.summitglobal.com/documents/Maxwell2012WaterMarketReview-a030912.pdf>.

Mc Neely, J.A., 1997. *Conservation and the Future: Trends and Options Toward the Year 2025*, IUCN. Available at: <http://books.google.com/books?hl=en&lr=&id=9G9d0CCjCjoC&pgis=1> [Accessed October 31, 2013].

Modern Water, 2010a. *CTM - Continuous Toxicity Monitoring - Early Warning System*, Available at: <http://www.modernwater.com>.

Modern Water, 2010b. 'Microtox CTM'. Available at: <http://www.modernwater.com/monitoring/toxicity/on-line-microtox-ctm>.

O'Halloran, R. *et al.*, 2009. *Current online water quality monitoring methods and their suitability for the western corridor purified recycled water scheme*, Available at: <http://www.urbanwateralliance.org.au/publications/UWSRA-tr10.pdf>.

O'Toole, G. *et al.*, 2000. 'Biofilm formation as microbial development'. *Annual review of microbiology*, 54, pp.49–79. Available at: <http://www.annualreviews.org/doi/pdf/10.1146/annurev.micro.54.1.49> [Accessed November 9, 2013].

Oki, T. & Kanae, S., 2006. 'Global hydrological cycles and world water resources'. *Science (New York, N.Y.)*, 313(5790), pp.1068–72. Available at: <http://www.sciencemag.org/content/313/5790/1068.short> [Accessed October 30, 2013].

Parvin, M. & Williams, J.G., 1975. 'The effect of temperature on the fracture of polycarbonate'. *Journal of Materials Science*, 10(11), pp.1883–1888. Available at: <http://en.wikipedia.org/wiki/Polycarbonate> [Accessed April 28, 2013].

Porex Inc., 2011a. 'PP Materials: Polypropylene (PP) Fibers, Plastics, & Plastic Material'. *porex.com*. Available at: <http://www.porex.com/technologies/materials/porous-plastics/polypropylene/> [Accessed April 28, 2013].

Porex Inc., 2011b. 'PVDF Material: Polyvinylidene Fluoride (PVDF) Material Properties'. *porex.com*. Available at: <http://www.porex.com/technologies/materials/porous-plastics/polyvinylidene-fluoride/> [Accessed April 29, 2013].

PRNewswire, 2010. 'Surgical Technologies; MedShape Solutions, Inc. Announces First FDA-cleared Shape Memory PEEK Device; Closing of \$10M Equity Offering'. *Medical Letter on the CDC & FDA*. Available at: <http://www.prnewswire.com/news-releases/medshape-solutions-inc-announces-first-fda-cleared-shape-memory-peek-device-closing-of-10m-equity-offering-60652462.html> [Accessed April 28, 2013].

Qian, S. & Bau, H.H., 2009. 'Magneto-Hydrodynamics Based Microfluidics'. *Mechanics Research Communications*, 36(1), pp.10–21. Available at: <http://www.pubmedcentral.nih.gov/articlerender.fcgi?artid=2768299&tool=pmcentrez&rendertype=abstract> [Accessed December 18, 2013].

Ramos, A., 2007. 'Microfluidic Technologies for Miniaturized Analysis Systems'. Available at: http://www.springer.com/cda/content/document/cda_downloaddocument/9780387285979-c1.pdf?SGWID=0-0-45-466112-p107950354.

Randles, N.J. & Gray, L.V., 2012. 'Consumable component kit'. Available at: http://worldwide.espacenet.com/publicationDetails/biblio?CC=US&NR=2012122138A1&KC=A1&FT=D&ND=3&date=20120517&DB=EPODOC&locale=en_EP.

Ren, K. *et al.*, 2011. 'Whole-Teflon microfluidic chips'. *Proceedings of the National Academy of Sciences of the United States of America*, 108(20), pp.8162–6. Available at: <http://www.pnas.org/content/108/20/8162.full> [Accessed March 12, 2013].

Ren, Z. *et al.*, 2007. 'The early warning of aquatic organophosphorus pesticide contamination by on-line monitoring behavioral changes of *Daphnia magna*'. *Environmental monitoring and*

assessment, 134(1-3), pp.373–83. Available at:

<http://www.ncbi.nlm.nih.gov/pubmed/17294269> [Accessed November 30, 2013].

Rice, E.W. *et al.*, 2012. *Standard Methods for Examination of Water & Wastewater Method* Assn Amer Public Health, ed., Available at: <http://www.amazon.it/Standard-Methods-Examination-Water-Wastewater/dp/0875530133>.

Roig, B. *et al.*, 2007. 'Application of ecotoxicological studies in integrated environmental monitoring: Possibilities and problems'. *TrAC Trends in Analytical Chemistry*, 26(4), pp.332–344. Available at: <http://www.sciencedirect.com/science/article/pii/S0165993606002664> [Accessed November 29, 2013].

Row Inc., 2011. 'PFA (Perfluoroalkoxy) Detailed Properties'. Available at: <http://www.row-inc.com/pfa.html> [Accessed April 29, 2013].

Ruby, E.G., *et al.*, 2005. 'Complete genome sequence of *Vibrio fischeri*: a symbiotic bacterium with pathogenic congeners'. *Proceedings of the National Academy of Sciences of the United States of America*, 102(8), pp.3004–9. Available at: <http://www.pnas.org/cgi/content/long/102/8/3004> [Accessed May 30, 2014].

Saias, L. *et al.*, 2011. 'Design, modeling and characterization of microfluidic architectures for high flow rate, small footprint microfluidic systems'. *Lab on a Chip*, 11(5), pp.822–832. Available at: <http://www.ncbi.nlm.nih.gov/pubmed/21240403>.

Sawyer, C. *et al.*, 2003. *Chemistry for Environmental Engineering and Science* 5th ed., McGraw Hill Book Co. Available at: <http://www.amazon.it/Chemistry-Environmental-Engineering-Science-Sawyer/dp/0072480661>.

Seedsofrainbow.wordpress.com, 2011. 'Hawaiian Bobtail Squid'. Available at: <http://seedsofrainbow.wordpress.com/2011/10/30/quorum-sensing-learning-about-lux-operons-of-vibrio-fischeri/> [Accessed May 13, 2013].

Shapley, J. *et al.* 2009. *Wax micro actuator*. GB2443261 (B) [Patent].

Shin, J.Y. *et al.*, 2005. 'Chemical structure and physical properties of cyclic olefin copolymers (IUPAC Technical Report)'. *Pure and Applied Chemistry*, 77(5), pp.801–814.

Available at: <http://www.iupac.org/publications/pac/77/5/0801/> [Accessed November 22, 2013].

Snogren, R.C., 1974. *Handbook of Surface Preparation*, New York: Palmerton Publishing Co. Available at: <https://en.wikipedia.org/wiki/Polyoxymethylene> [Accessed April 29, 2013].

Solvay Plastics Inc., 2014. 'Torlon® PAI'. Available at: http://www.solvayplastics.com/sites/solvayplastics/EN/specialty_polymers/Spire_Ultra_Polymers/Pages/Torlon.aspx [Accessed April 29, 2014].

Sonneveld, E. *et al.*, 2005. 'Development of androgen- and estrogen-responsive bioassays, members of a panel of human cell line-based highly selective steroid-responsive bioassays'. *Toxicological sciences : an official journal of the Society of Toxicology*, 83(1), pp.136–48. Available at: <http://www.ncbi.nlm.nih.gov/pubmed/15483189> [Accessed November 30, 2013].

Stein, R.S. & Misra, A., 1980. 'Morphological studies on polybutylene terephthalate'. *Journal of Polymer Science: Polymer Physics Edition*, 18(2), pp.327–342. Available at: <http://doi.wiley.com/10.1002/pol.1980.180180215> [Accessed December 6, 2013].

Steinwall Inc., 2012. 'PBT'. Available at: <http://www.steinwall.com/ART-PBT.html> [Accessed April 28, 2013].

Stevens, A.M. & Greenberg, E.P., 1997. 'Quorum Sensing in *Vibrio fischeri* : Essential Elements for Activation of the Luminescence Genes'. *Journal of Bacteriology*, 179(2), pp.557–562. Available at: <http://jb.asm.org/content/179/2/557.abstract>.

Stolper, P. *et al.*, 2008. 'Whole-cell luminescence-based flow-through biodetector for toxicity testing'. *Anal Bioanal Chem*, 390(4), pp.1181–1187. Available at: <http://www.ncbi.nlm.nih.gov/pubmed/18157666>.

Sullivan, C., 2002. 'Calculating a Water Poverty Index'. *World Development*, 30(7), pp.1195–1210. Available at: <http://www.sciencedirect.com/science/article/pii/S0305750X02000359> [Accessed October 27, 2013].

Swift, S. *et al.*, 1996. 'Quorum sensing: a population-density component in the determination of bacterial phenotype'. *Trends in Biochemical Sciences*, 21(6), pp.214–219. Available at:

<http://www.sciencedirect.com/science/article/pii/S0968000496800181> [Accessed November 30, 2013].

Tchobanoglous, G. & Schroeder, E.E., 1985. *Water quality: Characteristics, modeling, modification*, Prentice Hall. Available at: <http://www.amazon.com/Water-Quality-Characteristics-Modeling-Modification/dp/0201054337> [Accessed November 2, 2013].

TechSci Research, 2013. 'China Water Purifier Market Forecast & Opportunities, 2018', p.100. Available at: http://www.researchandmarkets.com/research/lpd6dw/china_water.

TechSci Research, 2012. 'Global Water Treatment Chemicals Market Forecast and Opportunities, 2017 - market research report', p.70. Available at: <http://www.reportlinker.com/p0923300-summary/Global-Water-Treatment-Chemicals-Market-Forecast-and-Opportunities.html> [Accessed May 13, 2013].

The Lee Company, 2002. 'Lee micro-dispensing vhs-starter kit manual'. Available at: <http://www.theleeco.com/products.cfm/>.

Tian, W.-C. & Finehout, E., 2009. 'Microfluidic diagnostic systems for the rapid detection and quantification of pathogens'. In *Microfluidics for Biological Applications*. Boston, MA: Springer US, pp. 271–322. Available at: <http://www.springerlink.com/index/10.1007/978-0-387-09480-9> [Accessed June 5, 2014].

Titow, W., 1984. *PVC technology* 4th ed., London: Elsevier Applied Science Publishers. Available at: <http://books.google.com/books?id=N79YwkVx4kWC> [Accessed April 29, 2013].

Umezawa, Y. *et al.*, 2000. 'Potentiometric selectivity coefficients of ion-selective electrodes'. *Pure and Applied Chemistry*, 72(10), pp.1851–2082. Available at: http://www.iupac.org/publications/pac/pdf/2000/7210/7210pdfs/7210omezawa_1852.pdf.

United States Environmental Protection Agency, 2012. 'Water Quality Standards Review and Revision'. Available at: <http://water.epa.gov/scitech/swguidance/standards/rev.cfm> [Accessed November 2, 2013].

Vanrolleghem, P.A. & Dae Sung, L., 2003. 'On-line monitoring equipment for wastewater treatment processes: state of the art'. *Water Science & Technology*, 47(2), pp.1–34. Available at: <http://www.ncbi.nlm.nih.gov/pubmed/12636059>.

Wilkes, C.E. *et al.*, 2005. *PVC Handbook*, Hanser Verlag. Available at: <http://books.google.com/?id=YUkJNI9QYsUC&pg=PA414> [Accessed April 29, 2013].

Wong, T.-S. *et al.*, 2011. 'Bioinspired self-repairing slippery surfaces with pressure-stable omniphobicity'. *Nature*, 477(7365), pp.443–7. Available at: <http://dx.doi.org/10.1038/nature10447> [Accessed November 9, 2013].

World Health Organization, 2011. *Guidelines for drinking-water quality, fourth edition*, World Health Organization. Available at: http://www.who.int/water_sanitation_health/publications/2011/dwq_guidelines/en/index.html [Accessed May 13, 2013].

Wu, J., 2006. 'Biased AC electro-osmosis for on-chip bioparticle processing'. *IEEE Transactions On Nanotechnology*, 5(2), pp.84–89. Available at: <http://ieeexplore.ieee.org/articleDetails.jsp?arnumber=1605218> [Accessed December 20, 2013].

Wu, N. *et al.*, 2005. 'Surface study of block and graft copolymers of polystyrene-polydimethylsiloxane'. *Acta Polymerica Sinica*, 1(5), pp.44–50. Available at: http://en.cnki.com.cn/Article_en/CJFDTOTAL-GFXB200501026.htm.

Xiao-li, D. *et al.*, 2008. 'Research progress on application of photobacteria in toxicity testing of environmental pollutants'. Available at: http://en.cnki.com.cn/Article_en/CJFDTOTAL-HGGS200802004.htm.

Zeng, W.R. *et al.*, 2002. 'Preliminary studies on burning behavior of polymethylmethacrylate (PMMA)'. *Journal of Fire Sciences*, 20(4), pp.297–317. Available at: <http://cat.inist.fr/?aModele=afficheN&cpsidt=14365060> [Accessed April 29, 2013].

Zhao, L. *et al.*, 2009. 'Antibacterial coatings on titanium implants'. *Journal of biomedical materials research. Part B, Applied biomaterials*, 91(1), pp.470–80. Available at: <http://www.ncbi.nlm.nih.gov/pubmed/19637369> [Accessed November 25, 2013].

Zulkifli, A., 2011. *Polyamide Imide*, John Wiley & Sons, Inc. ISBN:
10.1002/9781118229064.ch2.